PERCHLORATE REDUCTION USING *AZOSPIRA ORYZAE* ENZYMES IN SYNTHETIC VESICLES

BY

JUSTIN M. HUTCHISON

THESIS

Submitted in partial fulfillment of the requirements
for the degree of Master of Science in Environmental Engineering in Civil Engineering
in the Graduate College of the
University of Illinois at Urbana-Champaign, 2012

Urbana, Illinois

Adviser:

Research Assistant Professor Julie L. Zilles

ABSTRACT

The combination of manmade materials and biological components to form perchlorate-reducing vesicles may address several of the limitations associated with current perchlorate treatment technologies. The vesicles have a membrane comprised of the synthetic polymer, PMOXA-PDMS-PMOXA (ABA), which is stable over several months and is able to incorporate membrane proteins such as the outer membrane pores (OmpF). As the vesicles are formed, they can encapsulate perchlorate-reducing enzymes such as perchlorate reductase (Pcr) and chlorite dismutase (Cld).

To investigate the use of the vesicles in the treatment of perchlorate, polymer vesicles were formed with and without OmpF using the film-hydration method. Lipid vesicles were also tested. The size and size distribution of the vesicles was determined using dynamic light scattering and transmission electron microscopy. The perchlorate-reducing activity of the vesicles was determined using a colorimetric methyl viologen assay. The activity of the enzymes was assessed in oxygen and oxygen free environments, in 10% glycerol, and in the presence of protease and protease inhibitors. The activity of the enzymes toward similar anions such as nitrate and sulfate were determined with a UV-absorbance NADH assay and endpoint analysis using capillary electrophoresis.

The lipid and polymer vesicles demonstrated similar abilities to reduce perchlorate. Perchlorate-reducing activity was higher in vesicles with OmpF versus vesicles without OmpF. The activity of the enzymes showed no deterioration in the presence of oxygen versus non-oxygen environments. Addition of 10% glycerol proved to be an effective stabilizing agent for enzyme activity. Protease treatment of the enzymes resulted in partial enzyme inactivation. Protease inhibitors afforded no protective effects and even decreased activity. Enzymes had activity with nitrate but not sulfate. Perchlorate and nitrate competed for limited electron donor; however, the enzymes' affinity for perchlorate was much higher than nitrate.

The polymer and lipid vesicles demonstrate perchlorate-reducing capabilities in drinking water relevant conditions. With optimization, the vesicles show potential to compete with current treatment technologies for perchlorate. More broadly, the application of the treatment technology could be applied to any type of contaminant in which there are microbial degrading enzymes. Enzymes are also not limited to a specific set. Multiple contaminant-degrading enzymes could be encapsulated at various ratios to achieve flexible treatment. The flexibility of this treatment could lead to contaminant-tailored treatment options for drinking water facilities.

ACKNOWLEDGEMENTS

I would like to thank my adviser, Julie L. Zilles for offering support in this work. I would also like to thank her research group for offering feedback and discussion on my research. In particular, I would like to thank Courtney Flores and Michelle Marincel Payne. They offered research advice and more importantly, helped me transition into my engineering education. I would also like to thank Don Cropek, Irene MacAllister, Clint Arnett, John Kelsey and Richard Grant from Construction Engineering Research Labs for the support, advice, and help offered over the course of this project. I want to acknowledge the Kuehn Fellowship at the University of Illinois and the Army 6.1 Basic Research program for providing my research assistantship during this work. Finally, and most importantly, I would like to thank my wife, Katie Hutchison, for her love. Her unfailing support is the greatest reason in my switching careers and returning to school.

TABLE OF CONTENTS

LIST OF FIGURES

LIST OF TABLES

LIST OF EQUATIONS

CHAPTER 1 - INTRODUCTION:

Evolution of the processes for water purification has led to higher quality and larger quantities of treated water; however, water remains to this day an integral component of society. The quality and quantity of our drinking water is continually threatened by numerous factors including weather, contamination, accessibility and excessive use [1]. These threats have resulted in recent shortages in the southeast and western regions of the United States. Recent shortages have demonstrated a need to conserve and protect limited supplies.

To protect our water supplies, I focus my research on the remediation of the contaminant perchlorate. The structure of perchlorate includes a central chloride anion surrounded by four oxygen atoms with a size of approximately 3.5 angstroms (Figure 1). Perchlorate carries a negative charge and in solid form is typically associated with a hydrogen ion or another monovalent cation such as ammonium, potassium, or sodium. Aqueous perchlorate dissociates readily. Perchlorate is extremely stable in the environment due to its high activation energy. Due to its stability and with an estimated 15.9 million kilograms of perchlorate introduced into the environment due to rocket, munitions, and missile use, perchlorate-contaminated drinking water has been detected throughout the United States using advanced analytical methods with an average range of 5 to 20 parts per billion [2, 3]. Of great concern, perchlorate contamination of groundwater at 600 mg/L has been found at military and industrial sites [4]. These elevated concentrations are similar to pharmacological treatment doses used in the 1950's [5]. Perchlorate has also been introduced into the environment through the application of nitrate fertilizers harvested from Chile, where naturally occurring perchlorate-contaminated soil results in drinking water contamination exceeding 100 µg/L [6].

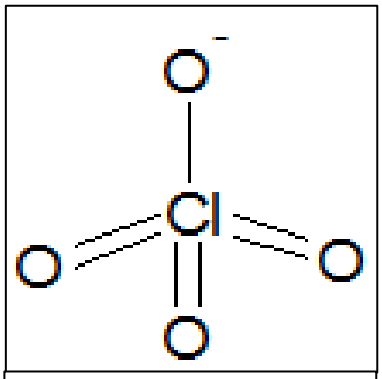

Figure 1: Chemical structure of the oxyanion perchlorate.

Perchlorate contamination of drinking waters is a growing concern with the development of advanced detection capabilities. These advanced techniques detect perchlorate contamination at parts per billion concentrations. At these low concentrations, scientists have begun to analyze the potential health effects on humans. Perchlorate affects human health by accumulating in the thyroid, resulting in iodide deficiency. The thyroid uses a sodium-iodide symporter to transport iodide into the thyroid, concentrating iodide at several orders of magnitude higher concentrations than the outside environment [7]. However, perchlorate uptake by the sodium iodide symporter is 30 times faster than the uptake rate of iodide [8]. Perchlorate interrupts the proper function of the thyroid which is essential to good health. The thyroid acts as a throttle for mammals, controlling several systems such as metabolic rate, production of proteins, rate of growth and the body's sensitivity to other hormones. The thyroid regulates these processes by producing hormones, predominantly triiodothyronine (T3) and thyroxine (T4). Iodide deficiency results in stunted growth and even mental retardation in fetuses and young children. In adults, iodide deficiency has been linked to hypothyroidism with common symptoms of fatigue, weight gain or difficulty losing weight, and muscle cramps [9].

These health effects arise from even short term or low dose exposure. Lamm et al. established a no-observed-adverse-effect-level (NOAEL) of absorbed perchlorate concentrations of 34 mg/day for adults [10]. Another study, from northern Chile, examined the effects of three perchlorate concentration ranges, 100 to 120 μg/L, 5 to 7 μg/L and <4 μg/L, on school children and newborns. Overall, the research claimed no observed suppressed thyroid function in newborns and school-age children from exposure to these dosages [6]. Large pharmacological doses in the range of 200 to upwards of 1200 mg/day were used in the 1950s to treat iodide-induced hyperthyroidism with successful results. Radioactive perchlorate inhibits the uptake of radioactive iodide into the thyroid [5]. However, few studies have directly measured the effects of perchlorate on sensitive populations within the United States [11].

Based on these studies, the Environmental Protection Agency (EPA) has decided to regulate perchlorate under the Safe Drinking Water Act. Initial assessments have recommended

perchlorate concentrations in drinking waters be limited to 15 µg/L [12, 13]. Once the EPA enacts a national drinking water standard, demand for perchlorate treatment will dramatically increase [14, 15]. Currently, some water facilities already treat for perchlorate using ion exchange or reverse osmosis. Demand for perchlorate treatment stems from increasingly strict state drinking water standards such as those in Massachusetts and the public perception of perchlorate's health effects [16].

The focus of my research is the development of a novel perchlorate remediation technology. This technology, called synthetic perchlorate reducing vesicles, combines manmade material and biological components. As shown in Figure 2, ABA polymer mimics cellular membranes and allows for the insertion of the biological *Escherichia coli* transport protein, outer membrane pore (OmpF). Perchlorate-degrading enzymes, perchlorate reductase

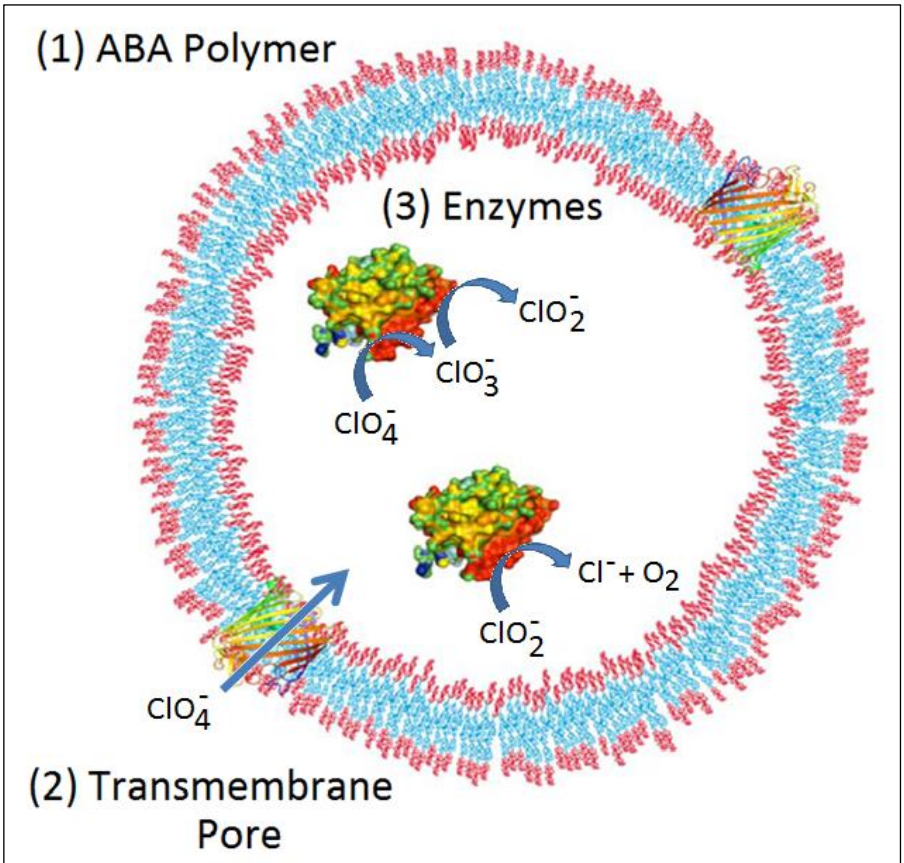

Figure 2: Synthetic Perchlorate Reducing Vesicle.
(1) One promising method for removing perchlorate from water is the use of PMOXA-PDMS-PMOXA ABA tri-block copolymer synthetic vesicles. (2) These synthetic vesicles mimic biological membranes by inserting pores such as OmpF, allowing perchlorate to diffuse into the vesicle. (3) Perchlorate-reducing enzymes, perchlorate reductase and chlorite dismutase, encapsulated in the vesicle degrade perchlorate into chloride and oxygen.

(Pcr) and chlorite dismutase (Cld), are encapsulated inside the vesicle. Perchlorate diffuses through the transmembrane pore into the vesicle. Once inside, perchlorate is degraded by the enzymes.

The vesicles are comprised of triblock copolymers that mimic the spherical structure of cell membranes with exterior hydrophilic and interior hydrophobic groups [17]. The polymer structure is poly-(2-methyloxazoline)-poly-(dimethylsiloxane)-poly-(2-methyloxazoline) ($PMOXA_{15}$-$PDMS_{110}$-$PMOXA_{15}$) (ABA) (Figure 3). The polymer has been shown to successfully insert other membrane proteins such as aquaporins and ATP synthase [18, 19]. ABA polymers naturally form vesicles, with the size of the vesicles dependent on the characteristics of the polymer's hydrophilic and hydrophobic block lengths [20]. These vesicles' wall on average is much thicker than liposome's walls and can range from 8-21 nm [21]. The stability of the vesicles is important for the long term use in water treatment. The vesicles' stability was studied using a variety of methods including size, size distribution, and permeability [22]. Permeability was measured using stopped-flow analysis and polymer vesicles showed less permeability than lipid vesicles [22]. For polymer vesicles in a water treatment relevant environment, the vesicles demonstrated stable size and size distribution for over a year.

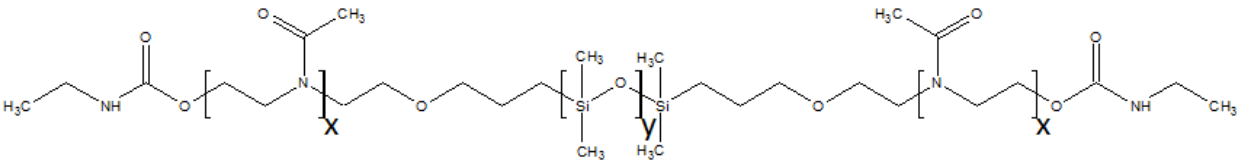

Figure 3: Chemical structure of the ABA polymer.
The polymer consists of repeating units of PMOXA and PDMS. Repeating units are indicated in brackets with x representing the number of PMOXA subunits and y PDMS subunits. Structures connecting the repeating units are referred to as blocks.

In addition to the polymer stability, vesicles offer other advantages over biological cultures. Perchlorate can be remediated by biological cultures; however, degradation is often limited by the presence of other electron acceptors such as oxygen and nitrate [23, 24]. Using contaminant-specific enzymes, the need for an anaerobic condition can be circumvented. Also,

as the vesicles are inert material, using the vesicles in drinking water applications may avoid the regulatory concerns associated with genetically modified organisms.

Introduction Summary: This thesis investigated the use of the perchlorate-reducing enzymes, perchlorate reductase and chlorite dismutase, in synthetic vesicles for treatment of perchlorate-contaminated water. The Literature Review details current treatment techniques for perchlorate remediation. These remediation techniques are classified into two categories, perchlorate separation and degradation technologies. The final treatment technology, biological reduction, segues into the discussion of perchlorate-reducing strain *Azospira oryzae*, the perchlorate-reducing enzymes' structure and capabilities, the enzyme purification, and our attempts at overexpression of the enzymes. The Materials and Methods outlines the procedures used to produce perchlorate-reducing vesicles and their analysis. Data is presented beginning with enzyme stability and anion degradation abilities followed by vesicles. The Discussion interprets the data to answer the hypothesis that synthetic perchlorate-reducing vesicles are capable of preferentially reducing perchlorate.

CHAPTER 2 - LITERATURE REVIEW

The first section of this literature review focuses on current treatment technologies for perchlorate-contaminated drinking water. By studying current perchlorate treatment technologies, limitations and difficulties associated with perchlorate treatment are elucidated. This information is utilized in this thesis to develop a perchlorate treatment technology that circumvents many of the current limitations. The final treatment technology, biological reduction, segues into the second section of the literature review, the biological enzymes responsible for perchlorate reduction. By studying the enzymes responsible for perchlorate degradation, information such as enzyme kinetics, enzyme requirements and anion competition can be optimized to improve the performance of synthetic perchlorate-reducing vesicles.

2.1: CURRENT TREATMENT TECHNOLOGIES FOR THE REMOVAL OF PERCHLORATE IN DRINKING WATERS.

With the recent announcement of the U.S. Environmental Protection Agency's intent to regulate perchlorate in drinking waters [25], research into drinking water detection and removal of perchlorate has increased. While no regulatory maximum contaminant level has been issued yet, it is anticipated that drinking water facilities throughout the United States may need to begin treating for perchlorate-contaminated waters. Several technologies are used to treat perchlorate-contaminated drinking water. These technologies are often divided into two categories: perchlorate separation and perchlorate degradation. Perchlorate separation technologies include granular activated carbon (GAC), membranes, and ion exchange, and their general function is described as pulling perchlorate anions out of drinking water. Technologies that degrade perchlorate include chemical and biological reduction and are defined by changing perchlorate into chloride in drinking water [26, 27]. In the following sections, I will outline the basic design and operation of each approach for the treatment of perchlorate in drinking waters.

2.1.1 Perchlorate Separation Technologies:

2.1.1.1 Granular Activated Carbon (GAC) – Absorption of contaminants into GAC is common throughout drinking water facilities in the United States. GAC typically used in drinking water facilities is a hydrophobic carbon compound. Due to its hydrophobic nature, activated carbon is typically used for non-volatile organic compounds. Activated carbon contains pores that contaminants enter and are trapped. The activated carbon is then removed for disposal or regeneration. Perchlorate, an inorganic anion, is generally not a candidate for treatment using virgin GAC. Using GAC technologies for the treatment of perchlorate requires that the GAC be altered into a more hydrophilic compound.

Modified GAC has been shown to successfully sorb perchlorate. Modifications of the GAC surface have included cetyltrimethylammonium chloride, iron oxalic acid and increasing the nitrogen content of GAC with ammonia [28-31]. These modifications increase the absorptive capacity of GAC and the breakthrough time for perchlorate. Despite the improvements in perchlorate sorption, the modifications are not without drawbacks. By altering GAC to sorb perchlorate, the carbon is susceptible to all inorganic anions. Also, organic non-volatiles are no longer sorbed to the activated carbon. Activated carbon also suffers drawbacks common in all perchlorate separation technology, including problems with regenerating the media and destruction of the concentrated perchlorate waste.

2.1.1.2 Membranes – Membrane technology relies on the use of a semi-permeable membrane that rejects the passage of molecules based on their physical properties such as size and polarity. Membranes are categorized by their pore structure, with the following names decreasing in pore size: microfiltration, ultrafiltration, nanofiltration and reverse osmosis. For smaller-pored membranes such as nanofiltration and reverse osmosis, water pressure is elevated on the influent side of the membrane compared to traditional drinking water treatment facilities to overcome the osmotic pressure barrier. Contaminants concentrate on the influent side of the membrane. Once

membranes become fouled, the membrane is washed and the contaminants are removed as a concentrated waste. For the anion perchlorate, microfiltration and ultrafiltration membranes are insufficient for perchlorate removal based on the anion size. Nanofiltration is capable of separating perchlorate from drinking water; however, reverse osmosis membranes have the highest perchlorate rejection rates [32].

For perchlorate removal from drinking water, membrane technologies have focused on two approaches. The first involves increasing the size of perchlorate through the use of polymers. Specialized polymers bind to perchlorate, increasing its diameter. This increased diameter prevents the passage of perchlorate through large-pored membranes such as ultra and microfiltration membranes [33, 34]. The other approach for perchlorate removal is the hindered diffusion of perchlorate through small-pored membranes such as nanofiltration and reverse osmosis. The small pore sizes and the amide bonds of the polymer membrane allow water to diffuse much more quickly across the membrane than perchlorate [35, 36]. A similar treatment relies on electricity rather than pressure to remove perchlorate: electrodialysis. This technique combines small-pored membranes that are cationic or anionic selective with an electrical current. Electrical current is applied to the water and perchlorate accumulates on the anionic selective membrane [26].

Despite the use of membrane technologies in drinking water treatment, the membranes suffer from numerous complications. The first method of perchlorate removal uses polymers which can be expensive and introduce unknown contaminants into drinking water. The second membrane method requires the use of pressure and electricity which increases the cost of perchlorate treatment. All of these approaches also generate large amounts of concentrated wastes that require additional treatment.

2.1.1.3 Ion Exchange – The basic principle of ion exchange is the introduction of a similar cation or anion into the drinking water in exchange for the target contaminant such as

perchlorate. This is accomplished by passing water through a column suitable for trapping ions. Ion exchange columns contain a variety of media, with most commercial columns containing organic polymers, such as polystyrene strands cross-linked by the addition of divinylbenzene. Other media includes zeolites, clay and humus. Media can be made mono or bifunctional. Bifunctional resins work to target a specific type of ions.

Varying functional groups are added to the polystyrene resin depending on the targeted contaminant. Functional groups are classified into four types: strongly acidic or basic or weakly acidic or basic. Strongly acidic and basic functional groups include sulfonic acid groups and quaternary ammonium groups respectively. For weakly acidic and basic functional groups, carboxylic acid groups and primary, secondary, or tertiary amino groups are used respectively. The resins are charged with innocuous or less hazardous ions that will be exchanged for the target contaminant. For anion exchange, resins are generally charged with hydroxide ions, monovalent anions, or polyvalent anions.

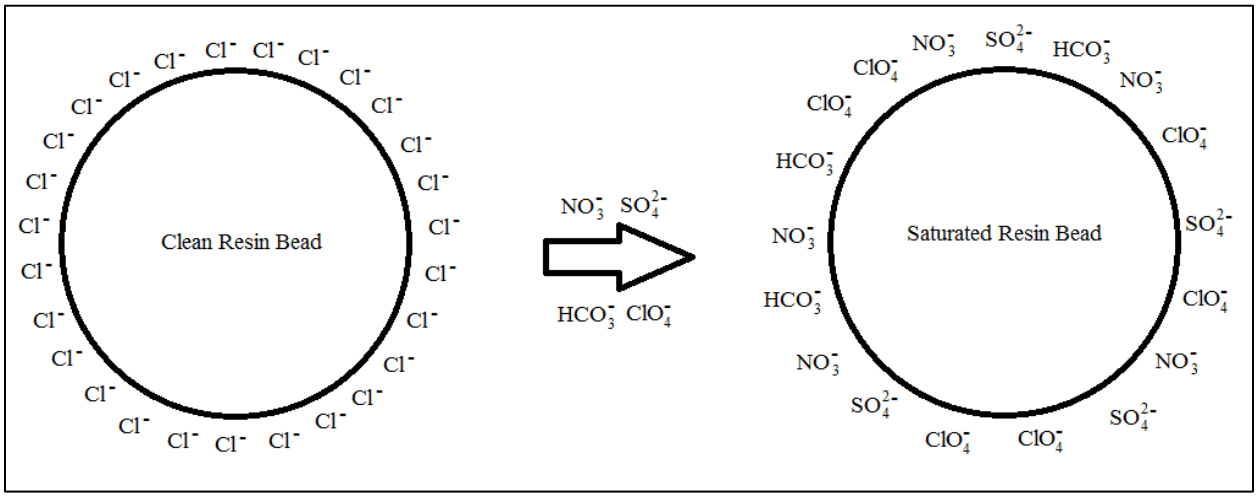

Figure 4: Ion Exchange Process for Perchlorate.
The above figure is an ion exchange process with perchlorate and other competing anions. A column filled with small clean resin beads (on the left) receives contaminated water. This water contains anions such as nitrate, sulfate, perchlorate, chloride and bicarbonate. These contaminants exchange places with chloride from the clean beads. Eventually, all beads in the column become saturated with non-chloride anions and must be regenerated or replaced for the system to continue removing anions.

The ion exchange process is similar for perchlorate treatment (Figure 4). However, treatment of perchlorate with ion exchange columns is often inefficient for two reasons. First, perchlorate in drinking water is in extremely low concentrations [26]. Second, several anions compete with perchlorate for resin sites. These anions include nitrate, chloride, sulfate and bicarbonate. Also, these competing anions are often at higher concentrations in drinking water than perchlorate [26].

To design an ion exchange system that effectively treats for perchlorate, resins were created to have a high selectivity (K_d) for perchlorate. The selectivity was created using a bifunctional resin with quaternary ammonium groups with long and short chains [37]. The long chains prevent larger anions such as nitrate and sulfate from interacting with the resin. Perchlorate, with low hydration energy, is sufficiently small to interact with the resin. The shorter chains increase the binding kinetics of perchlorate.

Over time, the functional sites of the resins become saturated with the target contaminant. Once the functional sites are saturated, perchlorate breakthrough will occur and target contaminant will appear in the effluent. Ion exchange columns can be recharged to prevent breakthrough. Regeneration of ion exchange columns occurs in three steps: backwashing, regeneration, and rinsing.

With the development of strong perchlorate-selective bifunctional resins, a new regeneration solution had to be developed since traditional anions such as chloride were unable to remove perchlorate. Scientists developed a two-step regeneration method involving anion displacement followed by an oxidation-reduction reaction. Tetrachloroferrate, a similar anion to perchlorate, was used to displace perchlorate from the resin [38]. Once the resin was saturated with the tetrachloroferrate, hydrochloric acid was used, causing the iron to release chloride. After two or more chlorides were released from the tetrachloroferreate, the compound became positively charged and dissociated from the resin due to charge repulsion. Chloride was then allowed to occupy and regenerate the resin. Single-use perchlorate selective resins have also successfully been used in the treatment of drinking water [39].

While ion exchange is a viable option for perchlorate treatment, several factors limit the effectiveness of the treatment. This includes competition of similar anions, including common anions such as sulfate and nitrate but also pentavalent arsenic, hexavalent selenium, and hexavalent chromium. Radionuclides such as uranium may also compete with ion exchange sites [40]. Another factor is the treatment of the concentrated wastes resulting from ion-exchange drinking water treatment. Treatment of the wastes is expensive involving high-energy processes including incineration and thermo-chemical conversion of the contaminants [41]. Alternative waste treatments such as microbial degradation have been developed but are also costly due to nutrient requirements of the bacteria.

2.1.2 Perchlorate Degradation Technologies:

2.1.2.1 Chemical Reduction – Chemical reduction of perchlorate is carried out through the transfer of eight electrons to the central chloride atom. Perchlorate is a strong oxidizing agent used in rocket fuels and munitions. Its degradation is thermodynamically favorable. However, perchlorate in the environment is very stable likely from the large kinetic energy required to provide the initial activation energy. This kinetic barrier is likely due to the inability to access the central chloride atom because of the surrounding four oxygen atoms in the tetrahedral structure.

Several studies have focused on the use of catalysts to decrease the activation energy required to degrade perchlorate. These catalysts have included palladium-rhodium carbon, methyloxerhenium oxides, titanium, titanium dioxide surfaces, and zero-valent iron. The first two catalysts are unlikely options for water treatment due to the harsh conditions required for the reactions. These conditions include extremely low pH, three or less [42-44]. Titanium presents reaction rates similar to biological degradation; however, complete perchlorate reduction requires the presence of hydrogen, an explosive gas [45]. Finally, zero-valent iron, acting as both catalyst and electron donor, has been shown to treat perchlorate-contaminated waters, but the kinetics of the reaction are too slow for practical applications [46-48].

Several other chemical reduction methods have also been studied for the reduction of perchlorate. Electrochemical conversion is possible but currently not practical due to similar disadvantages including slow degradation kinetics. Several studies reviewed in Srinivasan and Sorial [27] have attempted to determine the mechanism and kinetics of perchlorate degradation. These studies have included the use of numerous electrodes including platinum, technetium, rhenium, ruthenium, tin, and rhodium. Some general problems identified in these experiments include competitive inhibition of perchlorate degradation from similar anions such as chloride and sulfate [47]. As noted in ion exchange, these anions are typically found in much greater

concentrations in drinking water than perchlorate. The degradation process was also found to be too slow for practical use in drinking water facilities [49].

2.1.2.2. Biological Degradation – Biological degradation of perchlorate in laboratory, pilot scale and full-scale applications has been shown to successfully treat perchlorate [27]. The organisms responsible for perchlorate reduction were once thought to be a very limited group. However, perchlorate-reducing microbes have been found in a variety of environments and function very differently metabolically [50].

Nonetheless, trends have arisen out of perchlorate-reducing organism studies. For perchlorate reduction to occur, the bacteria require anoxic or anaerobic growth conditions. The presence of oxygen inhibits the use of perchlorate as the terminal electron acceptor [50-52]. Nitrate can also have a competitive influence on some perchlorate-reducing organisms [50, 51]. The metabolism of perchlorate degradation and detailed analysis of the enzymes responsible for degradation are discussed in the following section.

Full-scale treatment of perchlorate has been demonstrated in several non-drinking water sites. One of the first examples of perchlorate microbial degradation was conducted in fluidized bed reactors in California and Texas [53]. The reactors were able to successfully treat perchlorate contamination of 0.5 to 1 mg/L down to a non-detectable level of less than 4 µg/L.

One example of naturally-occurring perchlorate degradation includes the Salton Sea in California [54]. The Colorado River has perchlorate levels up to 4 µg/L. However, the Salton Sea, receiving Colorado River water, contains no detectable levels of perchlorate. It is thought that the seabed, with low dissolved oxygen, is an optimal environment for naturally-occurring perchlorate degradation.

While several examples for perchlorate degradation in engineered and natural systems exist, the technology has yet to be used in drinking water facilities for treatment of perchlorate contamination. This is mainly due to the public resistance or the aptly named "yuck" factor. The general public often takes issue with introducing bacteria to clean drinking water. Also, potential health effects could include elevated levels of chlorate or the toxic chlorite. Science has considerable work ahead to assure the public that the microbes present no adverse health implications.

2.1.3 Current Treatment Technologies Summary: Current treatment of perchlorate relies on the separation or degradation of perchlorate. Separation technologies, including granular activated carbon, membranes, and ion exchange, all suffer from similar drawbacks. The technologies are unable to target perchlorate specifically and require the disposal of concentrated waste. Adaptation of the current treatment technologies to target perchlorate specifically also has drawbacks. Modified GAC lacks perchlorate selectivity. Ion exchange resins modified for perchlorate can be difficult to regenerate. Perchlorate degradation technologies include chemical and biological degradation. Chemical degradation requires the use of heavy metal catalysts. The reaction kinetics for chemical perchlorate degradation are currently too slow for practical application in drinking water. Biological degradation requires an anaerobic environment due to competition with other preferential electron acceptors. Environmental conditions such as pH and temperature may need to be strictly controlled for optimal performance.

2.2: ENZYMES RESPONSIBLE FOR PERCHLORATE DEGRADATION.

The biological degradation of perchlorate is carried out through two enzymes, perchlorate reductase and chlorite dismutase (Figure 5). Perchlorate reductase catalyzes the reactions converting perchlorate into chlorate followed by conversion to chlorite. Chlorite dismutase converts the toxic chlorite into chloride and oxygen. Each enzyme is discussed below while

noting the metabolically unique nature of the enzyme perchlorate reductase and the distinctive reaction carried out by chlorite dismutase.

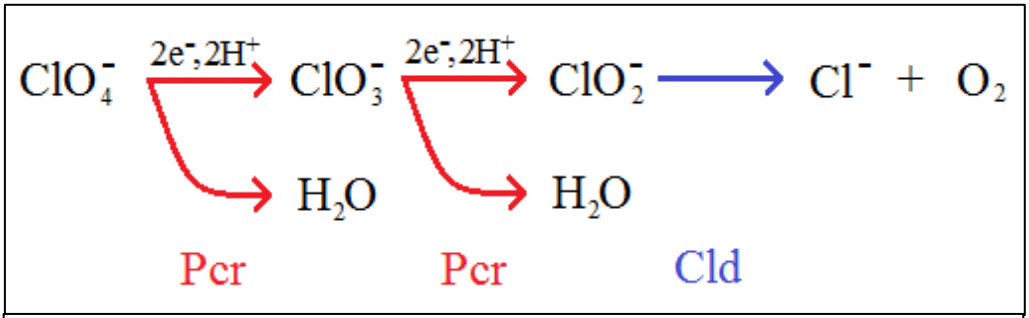

Figure 5: Enzymatic Conversion of Perchlorate.
The enzymes responsible for the conversion of perchlorate into chloride are perchlorate reductase (Pcr) and chlorite dismutase (Cld). Pcr transfers four electrons to the central chloride atom while releasing two water molecules. The final reaction, chlorite to chloride, involves an intramolecular exchange of four electrons between the oxygen and chloride atoms. This results in the separation of the molecule into chloride and diatomic oxygen.

For my research, the dissimilatory perchlorate-reducing organism, *Azospira oryzae* (synonym *Dechlorosoma suillum*) was used. This bacterium is a gram-negative rod, a nonfermentative facultative anaerobe and a part of the β subclass of *Proteobacteria*. The organism is unable to form spores and is motile by a single polar flagellum. The cells are capable of growing on simple organic fatty acids and use O_2, ClO_3^-, ClO_4^-, or NO_3^- as electron acceptors. Perchlorate and chlorate are fully oxidized to chloride and nitrate to nitrogen gas [55].

2.2.1 Perchlorate Reductase: Perchlorate reductases are metabolic enzymes allowing organisms to gain energy from the oxidation energy difference between electron donor and electron acceptor. The enzymes are membrane associated and require an electron donor such as acetate, methyl viologen, or nicotinamide adenine dinucleotide. Perchlorate reductase is a periplasmic-associated enzyme and a member of the type II dimethyl sulfoxide (DMSO) reductase family [56]. The enzyme can be divided into two categories. The first class of enzyme is capable of catalyzing both reactions, perchlorate to chlorate and chlorate to chlorite. The second class is only able to catalyze the reaction of chlorate to chlorite. Despite these differences, the enzymes all contain a molybdenum cofactor known as bis(molybdopterin guanine dinucleotide)-

molybdenum [57]. Perchlorate reductase has been shown to be a heterodimer or trimer of α, β, and γ subunits [56]. The α subunit contains the molybdenum cofactor. The β subunit contains an iron-sulfur cluster thought to be responsible for the electron transfer. The γ subunit is a cytochrome b moiety and is not present in all forms of perchlorate reductase. A final protein, δ, is thought to function as a chaperone protein in the formation of the α β heterodimer [56].

Purified perchlorate reductase from the strain GR-1, has been studied in the perchlorate reducing strain, GR-1[52]. This strain GR-1 was later determined to be *Dechlorosoma suillum*, a synonym of *A. oryzae*, through DNA hybridization [58]. This perchlorate reductase is a periplasmic enzyme. It has a molecular mass of 420 kDa and is comprised of a trimer of heterodimers ($\alpha_3\beta_3$). In addition to containing molybdenum, the subunits contain selenium [52]. Perchlorate reductase from *Dechloromonas aromatica* RCB overexpression and purification was attempted [59]. However, the enzyme was never successfully overexpressed as a result of deficient rare codons.

2.2.2 Chlorite Dismutase: This enzyme is responsible for the co-metabolic reduction of chlorite into chloride and oxygen. Accumulation of chlorite is toxic for organisms, and chlorite must be removed from the system when using perchlorate or chlorate as a terminal electron acceptor. Chlorite dismutase is a highly-conserved enzyme located in the periplasm of perchlorate-reducing bacteria [60]. The enzyme is the only known protein, aside from photosystem II, capable of forming diatomic oxygen [56]. Both oxygen atoms of the diatomic oxygen are thought to come directly from chlorite dismutase [61].

Chlorite dismutase has been purified from *Azospira oryzae* and is a homotetramer of 32 kDa subunits containing approximately one heme B (protoheme IX) per monomer [62]. The enzyme is very specific to chlorite, showing no enzymatic activity with hydrogen peroxide, perchlorate, chlorate, or nitrite [62]. Accumulation of chlorite in concentrations exceeding 225 mM results in loss of Cld activity, with diminished activity occurring in chlorite concentrations

exceeding 20 mM [62]. Chlorite dismutase has been heterologously expressed from *Dechloromonas aromatic* RCB in *Escherichia coli*. In these experiments, chlorite dismutase was shown to complete a limited number of reactions before suicidal inactivation. Approximately $1.7x10^4$ molecules of chlorite were degraded per active site [63].

2.2.3 Preparation of Enzymes for Use in This Study: Since only one of the enzymes, chlorite dismutase, has been successfully overexpressed in *E. coli*, *Azospira oryzae* lysates were used as the source of Pcr and Cld as previously described [52]. For the purposes of this study, cell lysates refer to cell extracts obtained after sonication. Soluble protein fraction refers to the enzymes that are separated by ultra-centrifugation from lipids.

CHAPTER 3 - MATERIALS AND METHODS

Preparation of OmpF Protein. To overexpress the *Escherichia coli* outer membrane protein, OmpF, the strain BL21(DE3) omp8 with the inserted hybrid plasmid pGEM-5Zf(+)-pET-3a, *ompF* (pGOmpF) was obtained from Dr. Meier's Lab in Basel, Switzerland [64, 65]. Purified protein was obtained using a previously described method [66] as follows. BL21(DE3) omp8 pGOmpF freezer cultures were streaked onto Luria-Bertani Lennox (LB) plates with 50 mg/L ampicillin (Amp) and incubated for 18 hours at 37°C. Individual colonies were immediately transferred. To assure retention of the plasmid, fresh plates directly streaked from -80°C were used. Three colonies were transferred to three 5 mL starter cultures and incubated with aeration at 37°C until growth reached an optical density at 600 nm of 0.6 (approximately 18 hours). Two of the starter cultures with optimal growth were each transferred to 1 L LB Amp broth and grown to an OD600 of 0.6 (approximately 6 hours). Cultures were induced with 0.4 mM Isopropyl β-D-thio-galactoside (IPTG) (Research Products International Corp., Mt. Prospect, IL) for six hours. Following induction, cells were pelleted at 5000xg for 15 min and stored at -80°C for up to three months. Prior to lysis, cells were thawed on ice and resuspended with 10 mL per gram wet cell weight of 20 mM Tris-Cl pH 8.0 with 1 U/mL DNase. (Roche Applied Science, Indianapolis, IN) Cell membranes were disrupted using a sonic dismembrator (Fisher Scientific Model 500 with Branson Tip Model 101-148-062, Waltham, MA). Three lysis cycles of five minutes alternating between a three second pulse at an amplitude of 35% and two seconds off, followed by five minutes on ice, were performed. Upon addition of freshly prepared 20% (w/v) sodium dodecyl sulfate (SDS) stock solution to a final concentration of 2%, the cell lysis solution clarified. The disrupted peptidoglycan layer and the associated OmpF were pelleted at 40000 x g for one hour at 4°C using a Beckman ultracentrifuge (Beckman-Coulter, Fullerton, CA). The pellet was washed three times with 5 mL of 20 mM phosphate buffer at pH 7.4 to remove traces of SDS. After washing, the lysate pellet was resuspended in 0.125% n-octyl-oligo-oxyethylene (octyl-POE) (Alexis Biochemicals, Farmingdale, NY) 20 mM phosphate buffer, pH7.4. The suspension was homogenized on ice using a manually operated Wheaton 7mL homogenizer followed by gentle stirring at 37°C for one hour, then centrifuged at 145,000 x g for 45 minutes at 4°C in a Beckman Ultracentrifuge. The cell pellet was resuspended in 3% Octyl-POE, 20mM

phosphate buffer at pH 7.4 and homogenized and centrifuged as before. Upon completion of the final centrifugation, OmpF protein remained suspended in the supernatant. Wash supernatants and OmpF were run on a 12% SDS Page gel at 120 V [67]. Bicinchoninic acid (BCA) (Pierce, Rockford, IL) assays were performed to determine protein concentration. OmpF protein was stored in sterile 1.5 mL microcentrifuge tubes at 4°C for up to three months.

Verify *Azospira oryzae* Identity. The identity of the *Azospira oryzae* ATCC number BAA-33 was verified by sequencing the 16S ribosomal RNA gene. DNA from the organism was extracted using the PowerSoil DNA Isolation Kit (Mo Bio, Carlsbad, CA). The polymerase chain reaction (PCR) reagents were obtained from a Qiagen Taq PCR Master Mix Kit (Qiagen, Valencia, CA) using standard 27 forward primer (5′-6-FAM-AGA GTT TGA TCM TGG CTC AG-3′) and 926 reverse primer (5'-CCG TCA ATT CCT TTA AGT TT-3'. Cycle conditions included an initial 95°C run for 3 minutes. This was followed by 30 cycles of 45 seconds at 94°C, 1 minute at 59°C and 2 minutes at 72°C. A final extension period was included at 72°C for 10 minutes. PCR product was purified using the QIAquick PCR Purification Kit (Qiagen, Valencia, CA). The sample was sequenced at the W.M. Keck Center for Comparative and Functional Genomics at the University of Illinois (Urbana, IL).

Preparation of *Azospira oryzae* Soluble Protein Fraction. *Azospira oryzae* ATCC number BAA-33 was purchased from ATCC (ATCC, Manassas, VA). Strains were stored in 30% glycerol stocks at -80°C. *A. oryzae* was grown using a previously published media [68] without the reductant and the hydrogen electron donor. Sodium acetate tri-hydrate was added to a molar concentration of 14.8 mM. Sodium perchlorate was added as an electron acceptor to a final concentration of 8.2 mM. A complete media list and order of preparation is included in Appendix A. Anaerobic test tubes containing 100 mL of media were capped with rubber stoppers and crimp sealed. The media was vacuumed three times with 80% nitrogen and 20% carbon dioxide mix for 10, 5 and 2 minutes with final pressure at 10 psi. Media was autoclaved and inoculated from the 30% glycerol freezer stock. Cells were grown to an OD600 of 0.4. Cultures were distributed into 9 mL aliquots with 1 mL glycerol. Culture stocks were stored at -

80°C for up to three months. Culture stocks were thawed at room temperature and transferred to a 2.5 L media prepared similarly in 5 L specialized anaerobic flasks (Chemglass, Vineland, NJ). Cells were grown to an OD600 of 0.6. Upon completion of growth, cells were harvested, pelleted and lysed in two different environments, anaerobic and aerobic. Anaerobic preparation was performed under N_2/H_2 headspace (49:1 v/v) in a COY anoxic glove box and sealed centrifuge tubes while aerobic preparations were performed on an open bench top. Soluble protein fractions were prepared similarly as previously described [52]. Cells were pelleted at 6000 x g for 10 minutes. Cell pellets were resuspended in 2 mL per gram wet weight cells of 50 mM potassium phosphate buffer, pH 6.0 with 0.1 mg/L DNase. After addition of the lysis buffer, cell membranes were disrupted using an amplitude of 35% on a sonic dismembrator (Fisher Scientific Model 500 with Branson Tip Model 101-148-062, Waltham, MA). Three lysis cycles of five minutes alternating between a three second pulse at an amplitude of 35% and two seconds off, followed by five minutes on ice, were performed. The cell extract was centrifuged at 5000 x g for 15 minutes at 4°C. 500 µL samples of the cell lysate supernatant were collected, treated with glycerol to a final concentration of 10% (v/v), and stored on ice for enzymatic analysis. The remaining cell lysate was centrifuged in a Beckman ultracentrifuge at 145,000 x g for one hour at 4°C to separate soluble protein from lipids. The soluble protein fraction was collected and tested for enzyme activity using the Methyl Viologen (MV) assay detailed below and protein content using BCA.

Perchlorate-Reducing Lysate Activity Assays using Methyl Viologen (MV). Enzymatic activity was analyzed using the electron shuttle MV, the electron donor sodium dithionite and the electron acceptor sodium perchlorate at room temperature (20°C) as previously described [52]. The buffer was purged of oxygen with 100% N_2 for thirty minutes. Headspace oxygen was removed with 100% nitrogen for five minutes. Reagents, sodium dithionite and perchlorate, were purged of oxygen for five minutes, and headspace oxygen was removed for one minute. For crude and purified lysates, 2 mL of assay mixture containing 0.5 mM of MV (Acros Organics, Pittsburgh, PA) in 50 mM Tris-Cl^-, pH 7.5 was added to anaerobic cuvettes (Helma, Mülheim, Germany) with cap and septa. 20 µL of cell lysate or soluble protein fraction was added and the sample blanked at 578 nm in a spectrophotometer. 1-5 µL of 0.2 M sodium

dithionite (Alfa Aesar, Ward Hill, MA) was added to achieve an initial absorbance of 1.8-2.0 at 578 nm. The sample was allowed to sit for 2-5 minutes to consume oxygen, and measurements were taken at room temperature until a level absorbance profile was achieved. 20 µL of 100 mM sodium perchlorate monohydrate (Fisher Scientific, Pittsburgh, PA) was added. The decreasing absorbance was measured until a zero value was achieved. The slope of the decreasing absorbance was calculated to determine activity. A similar procedure was used for vesicles, prepared as described below, except 400 µL of vesicles was added to the assay mixture and allowed to sit 10 minutes to consume oxygen before the addition of perchlorate. All samples were analyzed in a COY anoxic glove box to reduce oxygen exposure.

Endpoint Assays using Nicotinamide Adenine Dinucleotide (NADH) and Phenazine Methosulfate (PMS). To analyze endpoint concentrations of anions, a recently developed oxidation reduction reaction assay was used [69]. 50mM morpholinepropane sulfonic acid (MOPS) pH7.0 was placed in anaerobic bottled. The buffer was purged of oxygen with 100% N2 for 30 minutes. The bottles were capped with rubber stoppers and crimp sealed. Oxygen was removed from the headspace with 100% N_2 for 5 minutes. Buffer was autoclaved and stored in an anoxic glove box. NADH and PMS were added to the buffer to a final concentration of 1 mM and 100 µM respectively to obtain the assay mixture. Two mL of assay mixture were added to sealed vials along with 20 µL of cell lysates or soluble protein fraction. Perchlorate, nitrate, sulfate, and anion combinations were added at concentrations ranging from 100 to 500 µM. Reactions were allowed to proceed at room temperature for eight hours. Samples were frozen at -20°C to halt enzyme activity. Samples were filtered through a 0.22 µm syringe filter and analyzed as previously described [70] using capillary electrophoresis (CE). The system, Beckman Coulter P/ACE MDQ system (Beckman Coulter, Brea, CA), utilized a bare fused-silica capillary with an inner diameter of 75 µm and outer diameter of 375 µm. Samples were analyzed using running buffers provided in the Beckman Coulter Anion Analysis Kit, run at 20,000 volts with separation duration of ten minutes and detected using indirect UV detection set at 230 nm. Samples were also analyzed using ion chromatography on an Ion Pac AS-16 Hydroxide Selective Anion Exchange Column and an Ion Pac AS-18 Hydroxide-Selective Anion

Exchange Column on a Dionex ICS-2000 system (Dionex, Sunnyvale, CA) using 65 mM KOH eluent and a 1.2 mL/min eluent flow rate as previously described [71, 72].

Protease and Protease Inhibitor Treatment of Soluble Protein Fraction. The enzymes' susceptibility to the protease Proteinase K (Roche Applied Science, Indianapolis, IN) was analyzed. Cell lysates were prepared and treated with 5% (v/v) 20 mg/mL Proteinase K in double distilled water. The ratio of Proteinase K was adapted from RNA isolation [73]. The sample was incubated at room temperature for one hour. Protein content and enzyme activity were analyzed using BCA and MV assay respectively. Values were compared to negative control samples containing cell lysate and double distilled water. Protease inhibitors were also tested to determine their ability to limit the decline of perchlorate-reducing activity. The Complete Mini EDTA Free Protease Inhibitor Cocktail (Roche Applied Science, Indianapolis, IN) tablet was added to 10 mL of soluble protein fraction. Fractions were incubated at 4°C for 48 hours. Soluble protein fraction containing no protease inhibitor was incubated as a control.

Vesicle Formation with OmpF Insertion and Soluble Protein Fraction Encapsulation in Lipids and Polymer. Vesicles were formed using the previously published method of film rehydration [18]. The symmetric poly-(2-methyloxazoline)-block-poly-(dimethylsiloxane)-block-poly(2-methyloxazoline) ($PMOXA_{15}$-$PDMS_{110}$-$PMOXA_{15}$) was a gift from the Meier lab at the University of Basel, Switzerland and synthesized as published [17, 18]. Twelve milligrams of the polymer was dissolved in a 100 mL round bottom flask with 2 mL of chloroform. The chloroform was slowly removed using a Wheaton Rotary Vacuum Evaporator at room temperature under 100 mbar vacuum. Films were further dried under high vacuum of 5 mbar for 4 hours. Twenty milligrams of lipid with a 9:1 ratio of soy asolectin and cholesterol (Sigma-Aldrich, St. Louis, MO) were treated similarly to obtain a lipid single layer film. Two mL of soluble protein fraction and varying molar concentrations of purified OmpF were added to the round-bottom flask. The solution was mixed by alternating 30 second bath sonication and vortexing for 5 minutes. The mixture was stirred while stored at 4°C for 12 hours, sonicated and vortexed for an additional 5 minutes, and stirred while stored at 4°C for an additional 24 hours.

This treatment results in a cloudy, red mix that was then extruded through a 1 μm track-etched filter (Nucleopore, Whatman, GE Healthcare, Piscataway, NJ) in a LIPEX extruder (Northern Lipids, Burnaby, British Columbia, Canada). The solution was extruded an additional ten times through a 0.4 μm track-etched filter. To break up protein aggregates, the extruded unilamellar vesicles were treated with 5% (v/v) of 20 mg/mL Proteinase K for one hour at room temperature. To separate non-inserted OmpF, non-encapsulated protein and vesicles, size exclusion chromatography with a Sephacryl 500-HR column (GE Life Sciences, Piscataway, NJ) on a ÄKTAprime plus system (GE Life Sciences, Piscataway, NJ) was used with a maximum column pressure of 0.38 mPa and a flow rate of 0.5 ml/min [66]. Activity of encapsulated soluble protein fraction was measured with the MV assay and a vesicle volume of 400 μL. The vesicles size (diameter) and uniformity (polydispersivity index – PDI) were analyzed using dynamic light scattering (DLS) on a Zetasizer Nano ZS90 (Malvern Instruments Ltd., Malvern, UK) using a 632.8 nm He-Ne gas laser at 12.8° and 90°. Samples were analyzed using a refractive index of 1.47, absorption value of 0.10 and at room temperature. Reported values are an average measurement of three readings of the same sample.

Transmission Electron Microscopy (TEM). Transmission Electron Microscopy (TEM) was used to confirm formation of vesicles using a JEM-2100F TEM with LaB6 emitter (JEOL USA, Inc., Peabody, MA) located at the University of Illinois Material Research Laboratories (Urbana, Il.) Ultrathin holey carbon grids supported on gold mesh (Ted Pella, Inc., Redding, CA) were prepared for vesicle application by charging for 45 seconds under a Denton DPG-1 glow-discharge system (Denton Vacuum Inc., Moorestown, NJ) at 200 mA. Vesicle dilutions of 1:2 by volume in 50 mM phosphate buffer at pH 6.0 were used. Diluted vesicles were then incubated on the charged carbon grids for 2 minutes and then blotted. Grids were stained with 1% uranyl acetate dye (SPI, West Chester, PA) and immediately blotted. Grids were stained a final time for 1 minute and blotted. They were allowed to air-dry for five minutes. Grids were viewed at 200 kV and 110 μA e-beam current, and several images were acquired per grid at approximately 50k to 200k times magnification.

Permeability of Vesicles. Stopped-flow spectroscopy on a SX.17 MV spectrometer (Applied Photophysics, Surrey, UK) was used to determine permeability through the OmpF [74]. Prepared vesicles in 50 mM phosphate buffer at pH 6.0 were introduced to an equal volume of hyperosmotic solution of 1 molar sucrose or sodium chloride. The resulting shrinkage resulted in a change in the scattering of light that was measured and characterized as k. Dilutions of vesicles were tested 5-10 times. Tests were conducted at 10°C and 600 nm wavelength light. Light-scattering output for each test was averaged, normalized, and used with the following Equation 1 [74] to calculate vesicle permeability:

$$P_f = k/[(S/V_o) * V_w * \Delta_{osm}]$$

Equation 1: Permeability Equation.
Stopped flow analysis is used to calculate permeability using the above equation where P_f = permeability; k = initial rise or fall of light scattering fitted to an exponential rise equation; S/V_o = specific surface area of vesicles, where S is initial vesicle surface area and V_o is initial vesicle volume; V_w = molar volume of water, and Δ_{osm} = osmolarity gradient across the vesicle membrane. For sucrose, the Δosm was 1.0878 for a 1 molar solution [75].

OmpF Diffusive Transport and Vesicle Leakage Experiments in Lipids. Lipid films were produced as described in a previous section with 10 mg of lipids (7.108 mg of 1-palmitoyl-2-oleoyl-sn-glycero-3-phophocoline (POPC), 1.44 mg of 1-palmitoyl,2,oleoyl-sn-glycero-3-phophoethanolamine (POPE), and 1.45 mg 1,2-dioleoyl-sn-glycero-3-phosphate (DOPA) (Avanti Polar Lipids, Inc., Alabaster, Alabama) but were hydrated with 2 mL phosphate buffered saline (137 mM NaCl, 2.7 mM KCl, 4.3 mM $Na_2HPO_4 \cdot 7H_2O$, 1.4 mM KH_2PO_4) with 2 mM carboxyfluorescein (Life Technologies, Invitrogen, Carlsbad, CA) and 50:1 (w/w) OmpF. After size exclusion chromatography, sample fluorescence was measured on a SpectraMax Gemini (Molecular Devices, Sunnyvale, CA). Values were compared to a negative control sample without OmpF.

CHAPTER 4 - RESULTS

My work focused on the production of synthetic cells comprised of human-made and cellular components from two organisms: the artificially constructed ABA membrane polymer along with *Escherichia coli* and *Azospira oryzae* proteins. The purpose of these experiments was to determine the ability of these vesicles to reduce perchlorate. The Results chapter is divided into four sections: Perchlorate-Reducing Enzyme Production and Stability, Analytical Measurements of Anion Concentrations, Production of OmpF, and Formation and Analysis of Lipid and Polymer Vesicles. Understanding the stability of the enzymes under varying conditions is an important step in evaluating the potential use of these nano-vesicles for the reduction of perchlorate-contaminated drinking water, and the enzymes' ability to degrade perchlorate in the presence of competing anions would result in a dramatic improvement in perchlorate drinking water treatment. Maintaining activity would reduce the cost associated with operation. Finally optimizing OmpF overexpression and insertion ratios in polymer vesicles would allow for optimal diffusion of perchlorate into the vesicle for degradation.

4.1: PERCHLORATE-REDUCING ENZYME PRODUCTION AND STABILITY.

4.1.1 Confirmation of *Azospira oryzae* Culture: The perchlorate-reducing bacteria was verified by sequencing the 16S rRNA gene (Figure 6). Its identity as *Azospira oryzae* was confirmed by comparing sequences in the Ribosomal Database Project.

```
1    TCGAACGGCAGCACGGGAGCTTGCTCCTGGTGGCGAGTGGCGAACGGGTG
51   AGTAATACATCGGAACGTACCCAGGAGTGGGGGATAACGTAGCGAAAGTT
101  ACGCTAATACCGCATATTCTGTGAGCAGGAAAGCGGGGGATCGCAAGACC
151  TCGCGCTCTTGGAGCGGCCGATGTCGGATTAGCTAGTTGGTGAGGTAAAA
201  GCTCACCAAGGCGACGATCCGTAGCAGGTCTGAGAGGATGATCTGCCACA
251  CTGGGACTGAGACACGGCCCAGACTCCTACGGGAGGCAGCAGTGGGGAAT
301  TTTGGACAATGGGGGCAACCCTGATCCAGCCATGCCGCGTGAGTGAAGAA
351  GGCCTTCGGGTTGTAAAGCTCTTTCGGCGGGGAAGAAATGGCAACGGCTA
401  ATATCCGTTGTTGATGACGGTACCCGCATAAGAAGCACCGGCTAACTACG
451  TGCCAGCAGCCGCGGTAATACGTAGGGTGCGAGCGTTAATCGGAATTACT
501  GGGCGTAAAGCGTGCGCAGGCGGTTTCGTAAGACAGACGTGAAATCCCCG
551  GGCTCAACCTGGGAACTGCGTTTGTGACTGCGAGGCTAGAGTACGGCAGA
601  GGGGGGTAGAATTCCACGTGTAGCA
```

Figure 6: 16S rRNA Sequence.
The 5' to 3' ribosomal gene was amplified using polymerase chain reaction and sequenced. The sequence match score was 1.00.

4.1.2 Perchlorate-Reducing Enzyme Production: To obtain the perchlorate-degrading enzymes, perchlorate reductase and chlorite dismutase, growth of *Azospira oryzae* was performed as described [51]. Initially the organism grew well as determined by a previous graduate student [64]; however, during the transition to my work, the growth slowed considerably, with the organism taking up to 25 days to reach stationary phase. A new media (described in the Materials and Methods) was used and optical density was measured at 600nm to determine cell growth (Figure 7). The organism reached stationary growth around one day after inoculation. This allowed for large volumes of cells to be produced quickly, and the cells contained equivalent enzymatic activities as the previously published method (data not shown).

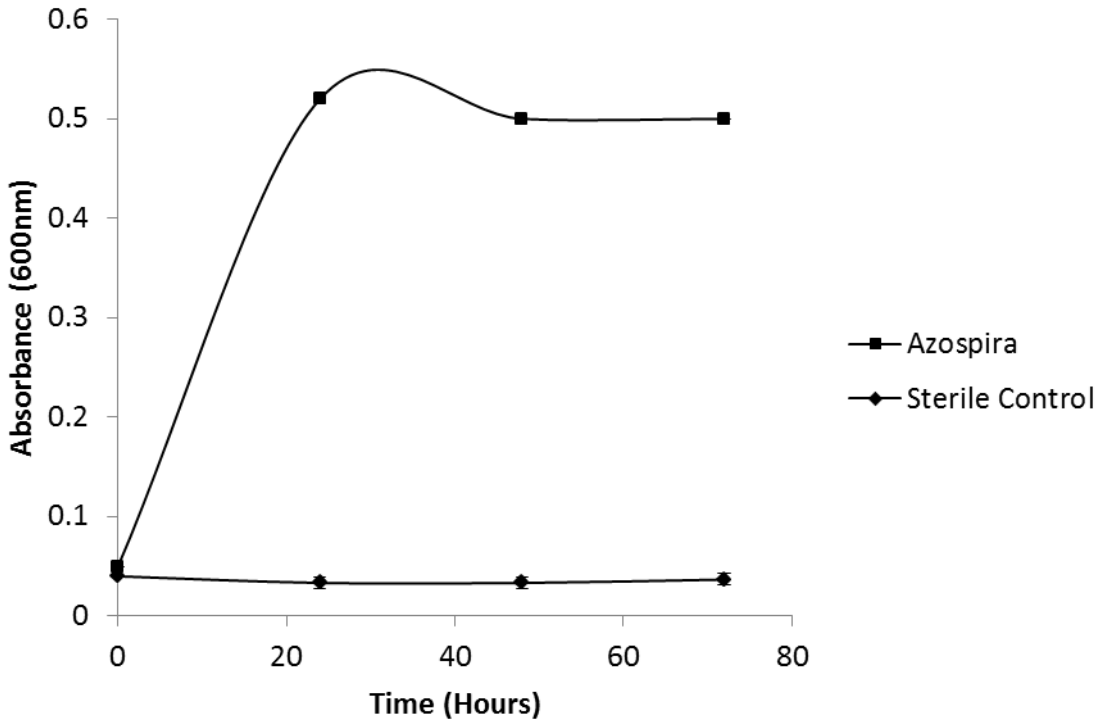

Figure 7: Growth of *Azospira.*
The sterile control was uninoculated media. Spectrophotometric measurements were taken at 600 nm. Experiments were performed with biological triplicates with negligible deviation. Error bars represent standard deviation.

To assure that cell growth corresponded to perchlorate reduction, time points were analyzed for perchlorate, chloride and acetate (Figure 8). Samples were taken starting at 0 hours; however, only samples starting at 23 hours have been analyzed. Chloride increases corresponding with growth of *Azospira oryzae* and conversion of perchlorate into chloride. Perchlorate and acetate decrease. Negative controls have only been performed once. The slight increase observed at early time points could correspond to measurement or dilution error.

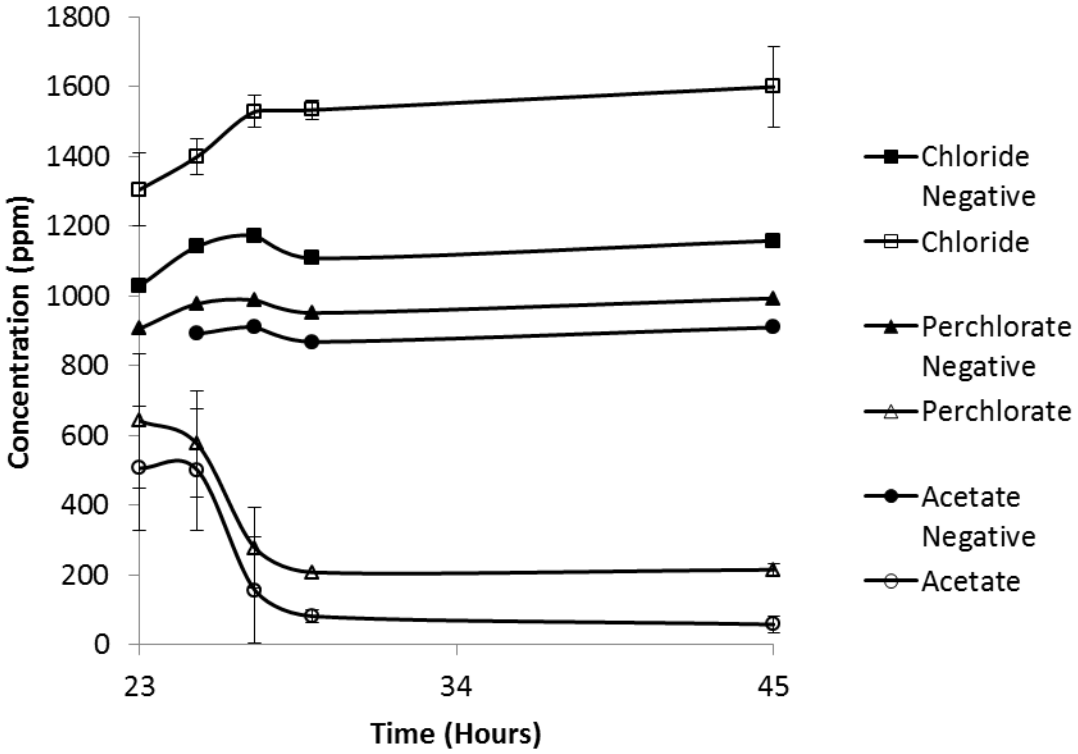

Figure 8: Dissimilatory Perchlorate Reduction.
Chloride, perchlorate and acetate were monitored. Dissimilatory perchlorate reduction and acetate consumption corresponded with cell growth as in Figure 7 and an increase in chloride concentration. Negative control was sterile growth media. Experiments except sterile controls were performed with biological triplicates. Capillary analysis was performed once on each sample. Error bars represent standard deviation.

Initially, ion chromatography was used to determine the perchlorate, nitrate and sulfate concentrations. This was met with a number of difficulties both my fault and hardware malfunction. In Figure 9, ion chromatograms are shown. In panel a, the chromatogram had a large peak at approximately 3.5 minutes corresponding to chloride concentration. It was later determined that this was due to adjustment of the buffer pH value using hydrochloric acid. In panel b, the chromatogram was noisy and contained no data of value. It was later determined that the influent tube on the column had a small leak. The leak was repaired; however in the meantime, I had switched to capillary electrophoresis, so all subsequent analyses were performed using the CE technique.

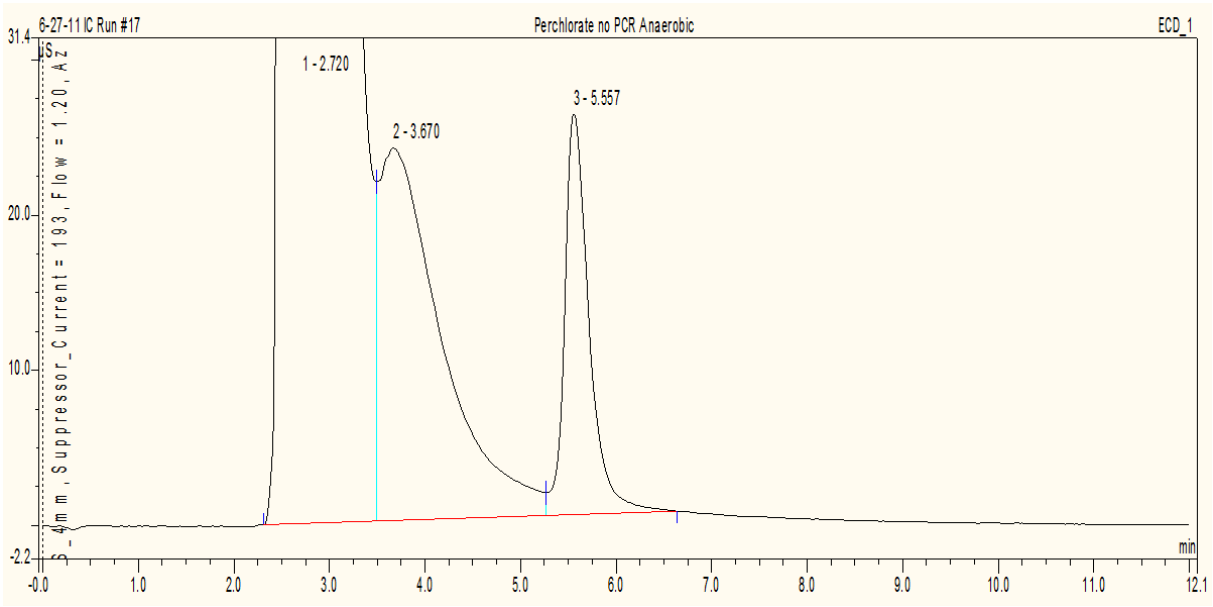

a

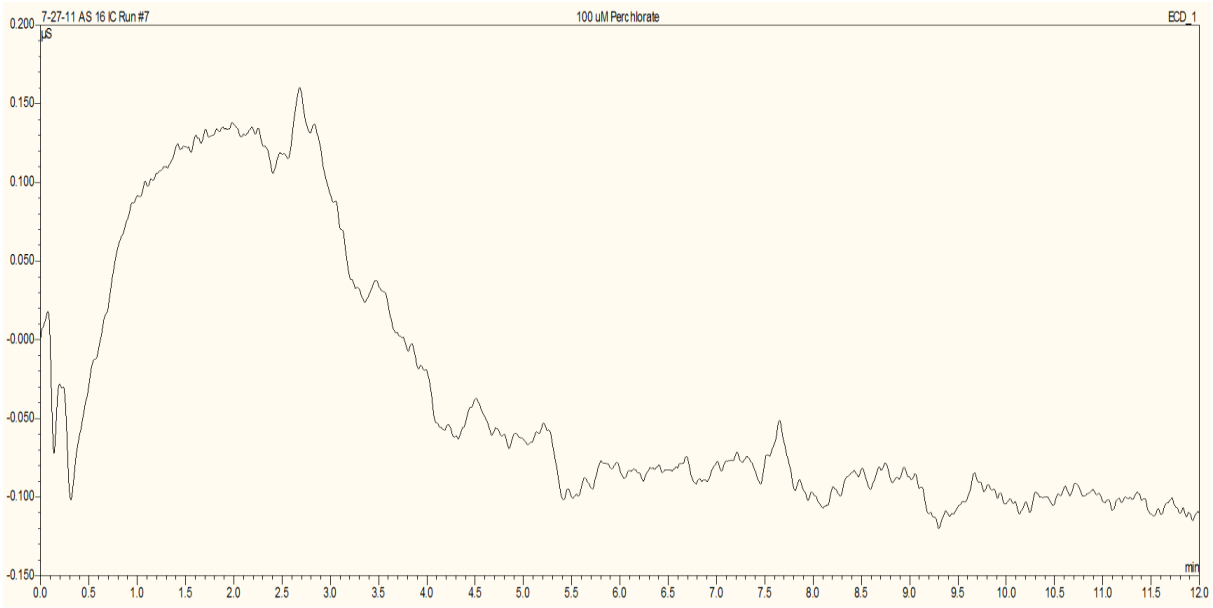

b

Figure 9: Ion Chromatography Analysis of Perchlorate.
a) Representative ion chromatogram of 100 µM perchlorate with no soluble protein fraction. The buffer used for ion chromatography analysis had pH adjusted with hydrochloric acid, resulting in a large chloride peak at approximately 3.5 minutes. **b)** Ion chromatogram with 100 µM of perchlorate in properly prepared buffer. The results are noisy with no discernible peak corresponding to perchlorate concentration. It was later determined that the influent tube on the column was leaking.

4.1.3 Enzyme Characteristics: Once perchlorate reduction was verified, the soluble protein fraction containing perchlorate-reducing enzymes, perchlorate reductase (Pcr) and chlorite dismutase (Cld), partially purified as described in the Materials and Methods section. The enzymes' functionality was then assessed under various conditions. These included aerobic versus anaerobic preparations, exposure to glycerol, and the introduction of protease and protease inhibitors. The enzymatic activities in this section were determined using the MV assay and 20 µL of cell lysate. Figure 10 shows a typical MV assay.

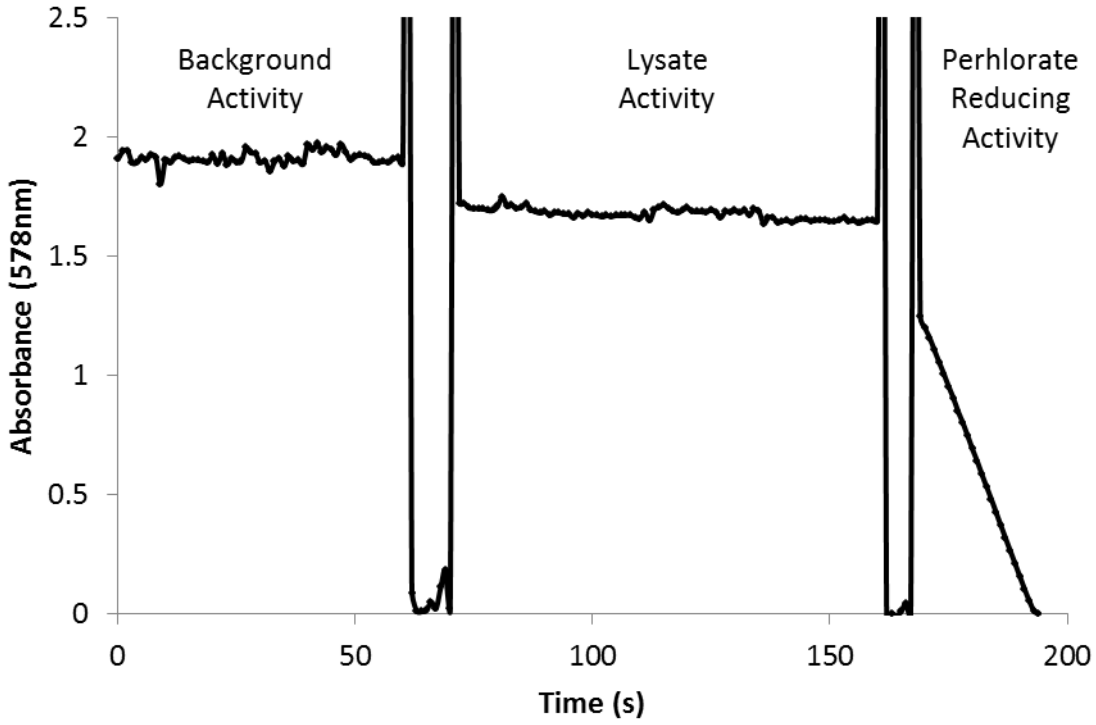

Figure 10: Typical Methyl Viologen Assay.
The background activity was analyzed from time 0-60 seconds. During this time, the methyl viologen scavenged oxygen from the reaction mixture. Lysate activity or soluble protein fraction, analyzed from 70-150 seconds, measured the intrinsic reducing power of the cell lysate. Perchlorate Reducing Activity, time 170-200 was measured upon addition of perchlorate. Large spikes and drops in the absorbance resulted from opening the spectrophotometer to add cell lysate or perchlorate.

For each test, the slope of the perchlorate-reducing activity was determined based on the oxidation of methyl viologen. Enzymatic activity was calculated from the slope and Equation 2 [76].

$$Activity\ \left(\frac{U}{L}\right) = \frac{\frac{AU}{min} * TV}{\varepsilon * b * SV} * 1000$$

Equation 2: Enzyme Activity.
The activity of the extract is defined as 1 µmole of reduced methyl viologen oxidized per minute, per liter of extract. The change in the slope of the absorbance with respect to minutes (AU/min), the total volume (TV) in µL, the µmolar absorptivity of methyl viologen (ε) with a value of 13.1 L/(mMol*cm) as previously determine [77], the path length (b) in centimeters, and the sample volume (SV) in µL were used to determine activity.

Enzymatic activities varied with respect to level of purification. Cell lysate preparations were in the range of 40,000 to 50,000 U/L. Activities for soluble protein fraction resulted in values in the range of 20,000 to 25,000 U/L. See Appendix B for a table summarizing the activities of individual tests. Using Equation 2 and the colorimetric MV assay, several environmental conditions were tested to study the enzymatic stability of Pcr and Cld.

4.1.4 Aerobic versus Anaerobic Lysate Preparation: Several studies offer conflicting results on oxygen sensitivity for the perchlorate-reducing enzymes. Aerobic storage of enzymes was reported to deteriorate activity of the enzymes with a half-life of two to three days in the *Azospira oryzae* GR-1 strain [52]. Other research showed a decrease in activity occurs in both aerobic and anaerobic conditions for enzymes from the organism *Dechloromonas aromatica*. [59]. To test whether aerobic preparation of the enzymes Pcr and Cld from *A. oryzae* was affecting activity in my experiments, I prepared cells lysates aerobically and anaerobically as described in the Materials and Methods section and compared the activity of each preparation. As shown in Figure 11, the enzyme activities were not significantly affected by the presence of oxygen (n=3 and P=0.439). Based on these results and the difficulty of anaerobic work, hydration, extrusion and exclusion of the perchlorate reducing vesicles was performed aerobically for all subsequent experiments.

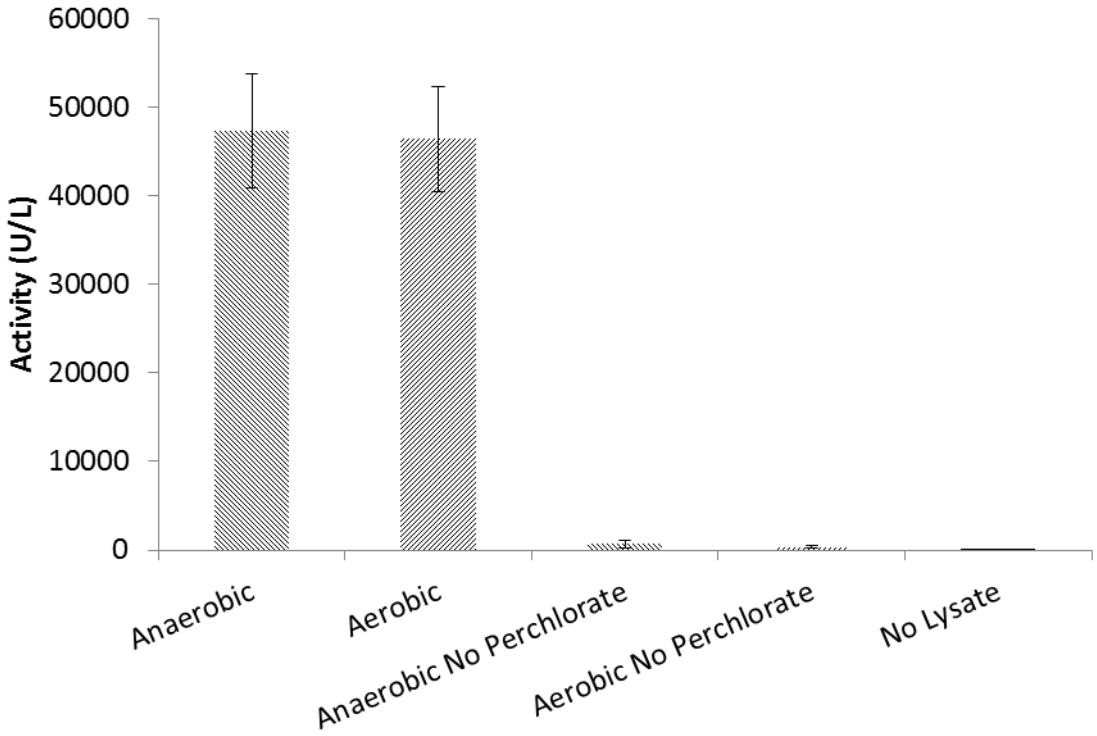

Figure 11: Anaerobic and Aerobic Cell Lysate.
The activity levels of cell lysate prepared anaerobically and aerobically show no statistically significant difference. Experiment was performed with biological triplicates and measurements in duplicate. Error bars are standard deviation.

4.1.5 Glycerol Stabilization of Enzymes: Adding glycerol to lysate has been shown to stabilize enzymes [51]. However, other sources report discrepancies with the benefits of glycerol addition [59]. The disagreement among the literature could be the result of using different strains of perchlorate reducers. As a result, it was important to test the benefits of glycerol on soluble protein fractions from *A. oryzae*. Addition of 10% glycerol did not affect the initial activity of the enzymes (n=3 P=0.388, Figure 12a) and slowed the half-life deterioration of the enzymes (n=3 P=0.000005, Figure 12b).

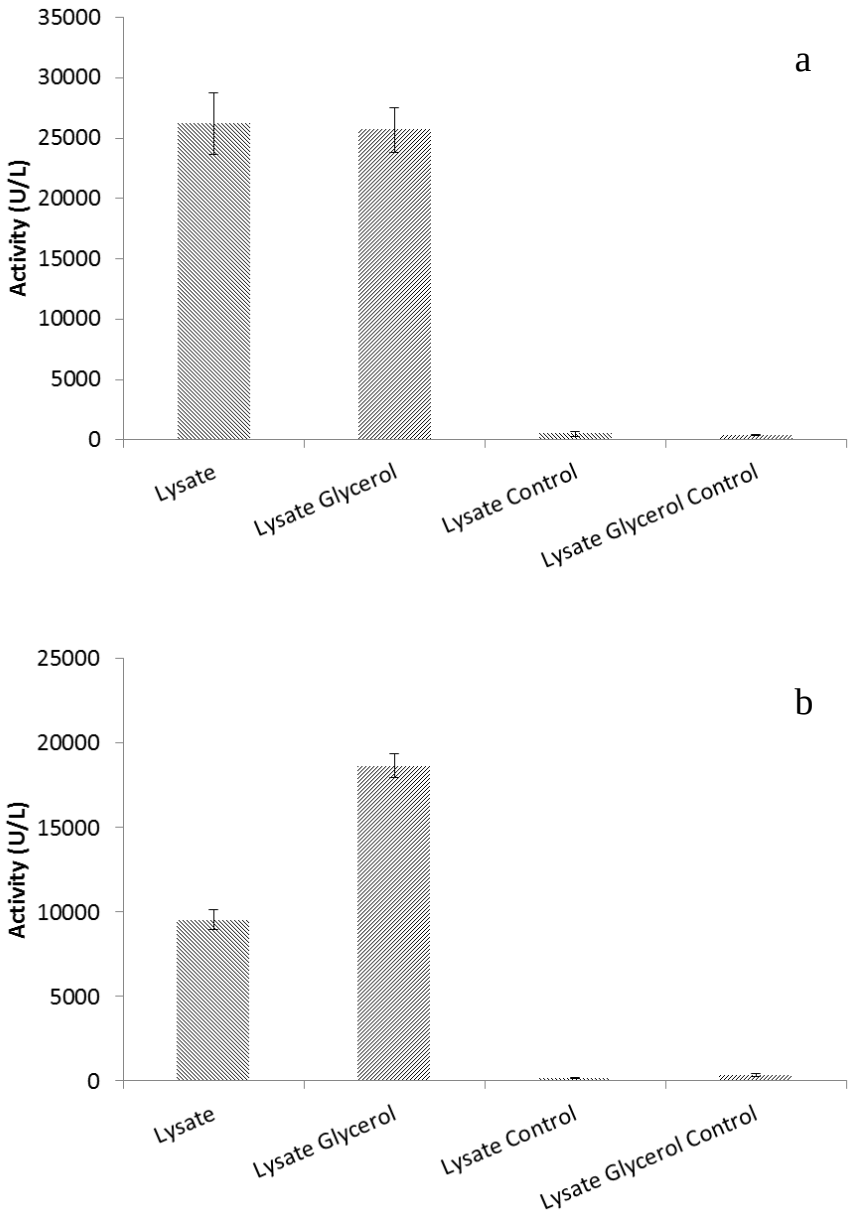

Figure 12: Effects of Glycerol on Activity.
a) Initial introduction of the glycerol does not affect the enzymatic activity. The activity of soluble protein fraction was determined using the MV assay and 20 µL of soluble protein fraction. Glycerol activity was adjusted for dilution. **b)** Lysate Glycerol sample was incubated with 10% glycerol at 4°C for 48 hours. Addition of glycerol, while not preventing all the deterioration of enzyme activity, significantly reduced the loss of activity. Experiments were performed with biological triplicates with duplicate measurements. Results are not statistically different. Experiments were performed with biological triplicates with duplicate measurements. Results are statistically different with error bars representing standard deviation.

4.1.6 Native Protease Degradation of Enzymes Pcr and Cld: To assess whether the loss of soluble protein fraction activity over time was the result of native proteases, soluble protein fractions were treated with a broad spectrum protease inhibitor, the Roche Applied Science Complete Mini Protease Inhibitor Cocktail (Figure 13). However, lysates treated with protease inhibitor showed reduced activity. This was unexpected but could be the result of the inhibition of a native protease responsible for protecting the perchlorate-reducing enzymes.

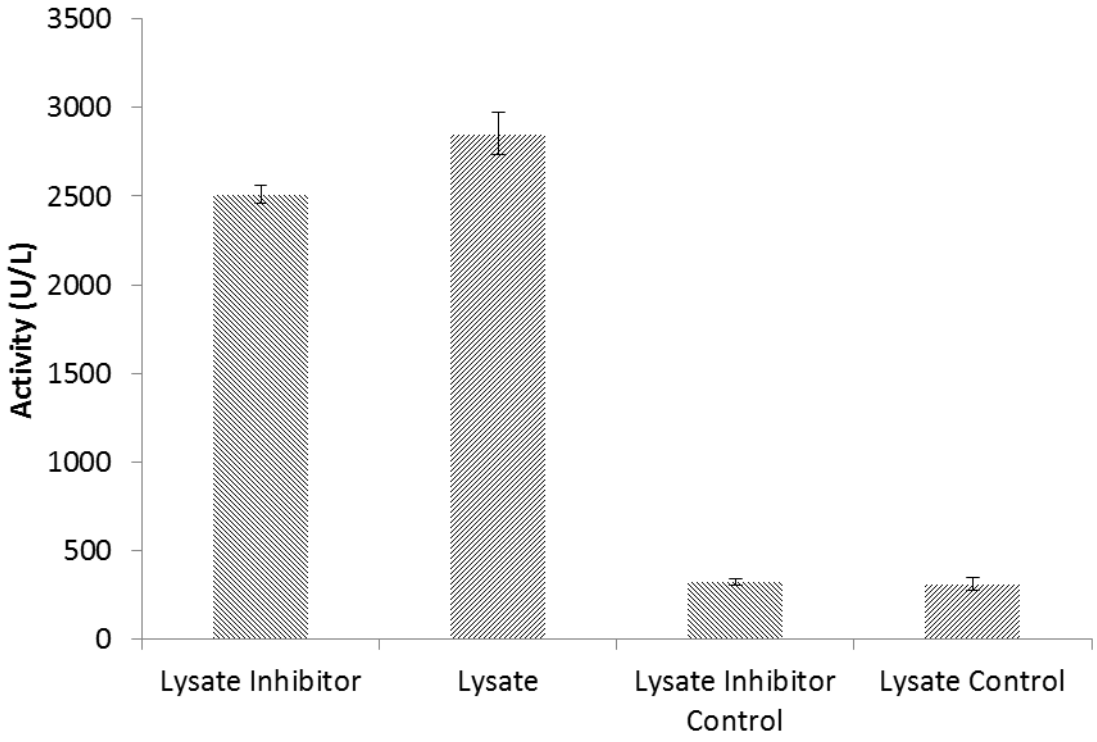

Figure 13: Native Protease Degradation of Soluble Protein Fraction.
Protease inhibitors were included in soluble protein fraction in order to prevent the decline of enzymatic activity. Activities for the enzymes are shown after addition of protease inhibitor and incubated for 48 hours at 4°C. Protease inhibitor was added directly to the soluble protein fraction at 10 mg per 1 mL respectively. Assay results were determined using 20uL of soluble protein fraction with reduced enzymatic activity due to extended storage. Experiments were performed with biological duplicates with single measurements. Error bars represent standard deviation.

4.1.7 Simulated Microbial Degradation: To simulate microbial degradation, the soluble protein fraction was treated with the protease, Proteinase K. This simulated microbial degradation was also used later to test the protective abilities of the lipid and polymer vesicles. The initial

activities in this experiment were reduced because of extended storage. Treatment with proteases for one hour at 25°C resulted in significantly reduced activity (n=3 P=0.021, Figure 14). However, substantial activity remained in the treated cell lysate. This could be the result of adaptation of the cytoplasmic RNA preparation protocol. While the ratio of Proteinase K to soluble protein fraction is similar to the protocol, the concentration of the Proteinase K and soluble protein fraction is higher. In addition, the cited protocol calls for Proteinase K treatment of fifteen minutes at 37°C whereas my experiments were conducted for one hour at 25°C.

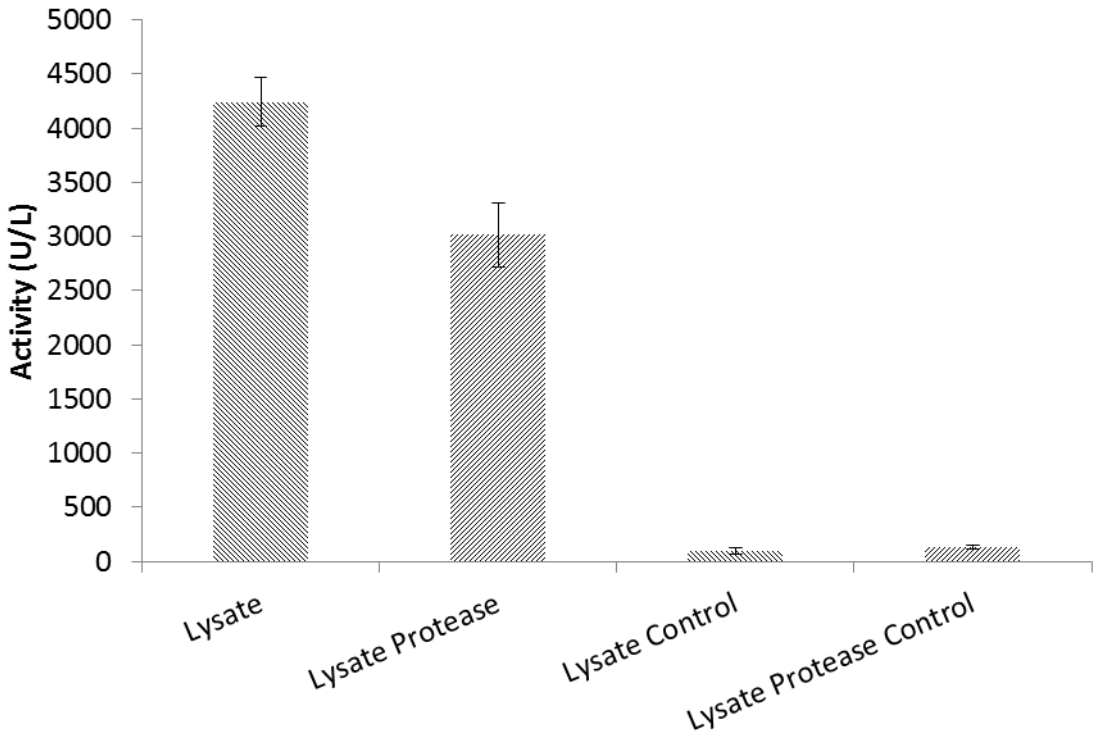

Figure 14: Protease K Reduces Enzyme Activity.
The above figure demonstrates the enzymes' susceptibility to Proteinase K. The protease was used to simulate microbial degradation. Protease was added to the soluble protein fraction at 5% v/v with the control, Lysate, only having 5% v/v double distilled water. Assay activity was determined using 20 µL of soluble protein fraction. Experiments were performed in triplicate with duplicate measurements. Results are statistically different with error bars representing standard deviation.

4.2: ANALYTICAL MEASUREMENT OF THE SOLUBLE PROTEIN FRACTION'S ABILITY TO REDUCE ANIONS.

The following section focuses on the analytical measurement of the conversion of perchlorate to chloride. The purpose of these experiments is to assure complete conversion of perchlorate to chloride, as the formation of chlorite is toxic. As mentioned in the introduction, perchlorate treatment technologies are often hindered by the presence of similar anions which are often in greater concentrations than perchlorate. Data on the enzymes' activity toward other anions are presented. Soluble protein fractions were incubated with varying concentrations of anions using the NADH assays as described in the Material and Methods Section. The NADH assay was published by another lab [69] during this thesis and proved to be more consistent than the methyl viologen assay in the presence of oxygen. For this reason, the NADH assay was used for anion competition analysis.

4.2.1 Stoichiometric Conversion of Perchlorate to the Chloride Anion: To test that one mole of perchlorate was converted to one mole of chloride, varying concentrations of perchlorate were incubated with the soluble protein fraction in the presence of excess or limiting NADH concentrations. Electrons donated to the reduction of perchlorate into chlorate and chlorate to chlorite can be directly measured using spectrophotometric methods utilized by the MV and NADH assays. Conversion of chlorite required no external electron donor. Chlorite conversion was indirectly measured through the formation of diatomic oxygen, which is capable of accepting electrons from MV and NADH. Endpoint assays were performed to assure complete conversion of perchlorate to chloride.

In Figure 15, varying concentrations of perchlorate were converted to chloride in near 1:1 molar ratio. Assay results showed no intermediate formation of chlorate or chlorite. These results extended to reactions with limited NADH concentrations. Perchlorate incubated with the

minimum NADH requirement to convert perchlorate to chlorite resulted in near complete conversion of perchlorate to chloride with no intermediate chlorate or chlorite present.

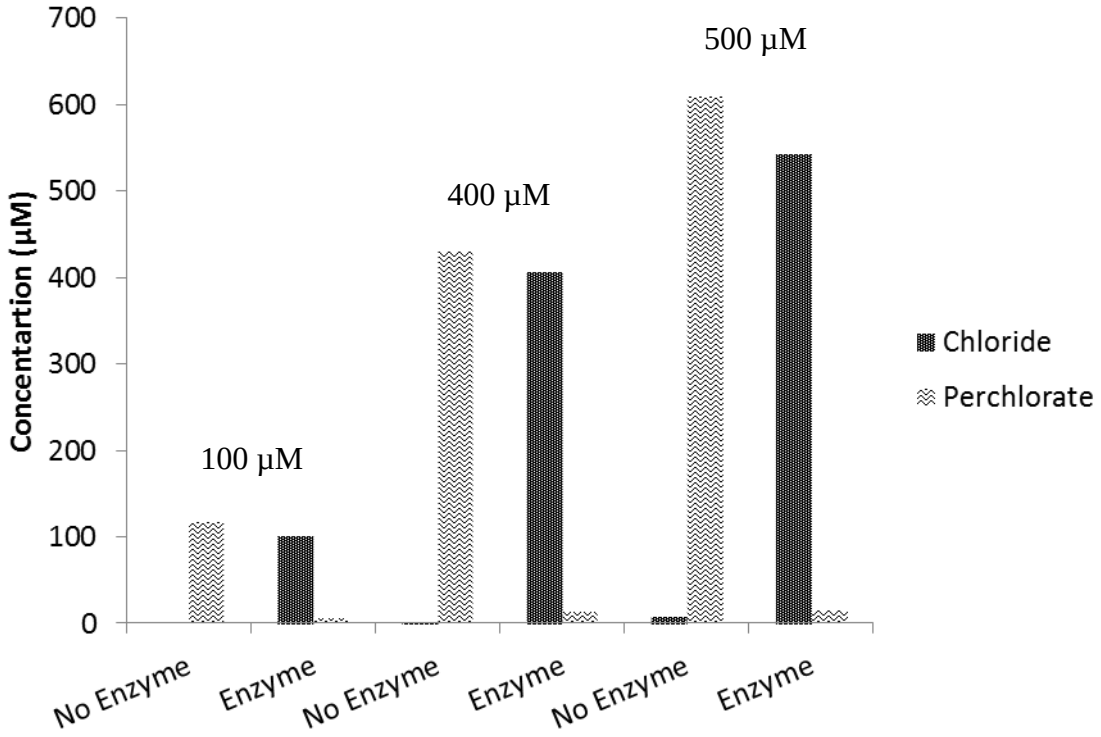

Figure 15: Stoichiometric Conversion of Perchlorate to Chloride.
The conversion of perchlorate resulted in a near one to one molar conversion. Three experiments were conducted. The first and second include 100 µM and 400 µM of perchlorate with and without soluble protein fraction containing perchlorate-reducing enzymes and excess NADH. The third contains 500 µM perchlorate and enough NADH to convert perchlorate to chlorite. This indicates the both the perchlorate-reducing enzymes, Pcr and Cld, were functional converting perchlorate to chloride. Assays were performed with 20 µL of soluble protein fraction. Assays were performed with one biological sample.

4.2.2 Reduction of Similar Anions by Pcr and Cld: In addition to studying the reducing ability of the *A. oryzae* enzymes for perchlorate, sulfate and nitrate were analyzed (Figure 16). For many of the current perchlorate-treatment technologies, similar anions such as nitrate and sulfate present inhibitory effects. Reduction of the anions was coupled to NADH as the electron donor. The soluble protein fraction was capable of reducing nitrate as previously published for *A. oryzae* [52]. The results did not show the formation of another anion such as nitrite. Nitrate was converted to an unknown compound; however, from previous research, nitrate is likely converted to nitrogen [51]. Sulfate was not reduced. An increase in sulfate concentration occurs because of the addition of the sulfate-containing soluble protein fraction.

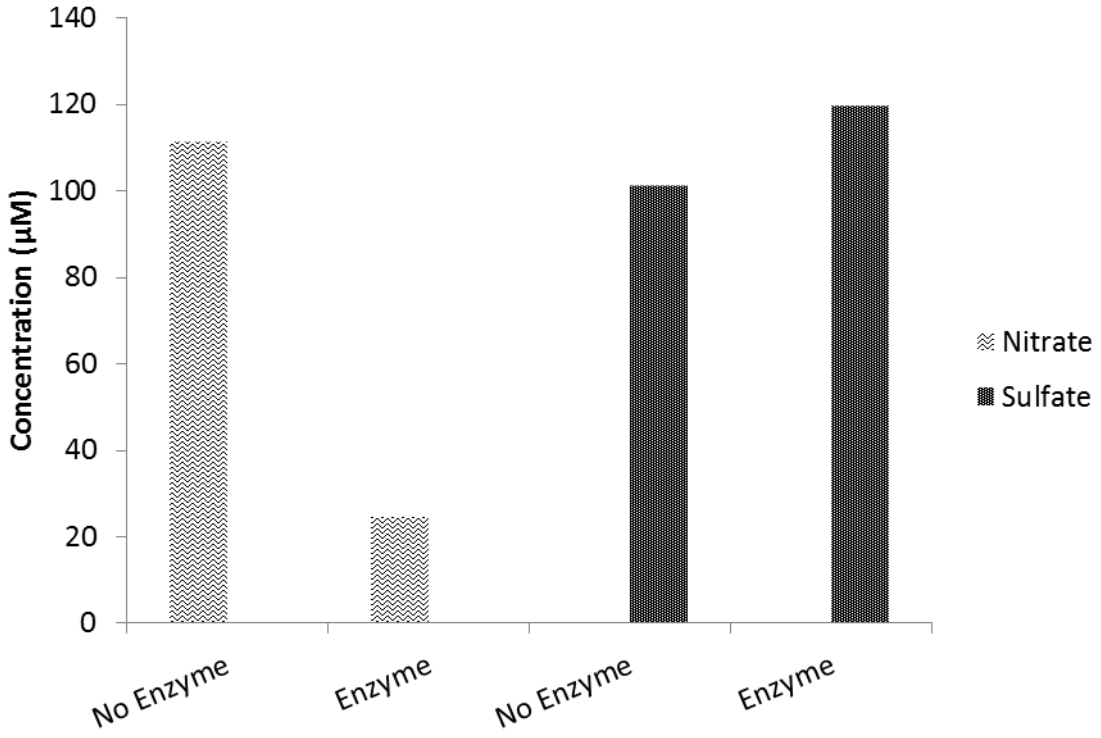

Figure 16: Soluble Protein Fraction's Ability to Reduce Similar Anions.
This figure demonstrates the ability of the soluble protein fraction to reduce nitrate. Anions were added at a concentration of 100 µM with 20 µL of soluble protein fraction. Residual concentrations of nitrate could suggest that the process requires more than 5:1 molar ratio of NADH or the soluble protein fraction was unable to degrade minimal nitrate concentration. Sulfate was not reduced. An increase in sulfate concentration with the addition of soluble protein fraction is due to the sulfate concentration in the enzymes. Assays were performed with one biological sample.

4.2.3 Competitive Reduction of Similar Anions: Knowing that the enzymes had activity with nitrate, anion mixtures were incubated with the soluble protein fraction to determine if sulfate and nitrate had inhibitory effects on perchlorate degradation. Sulfate had no inhibitory effect on perchlorate end-point degradation and was not degraded by the enzymes (Figure 17). Apparent sulfate decreases in the 100 µM and the 400 µM are thought to be part of a matrix effect as sulfate and perchlorate elute at the same time. Samples were analyzed using NADH as electron donor with 20 µL of soluble protein fraction.

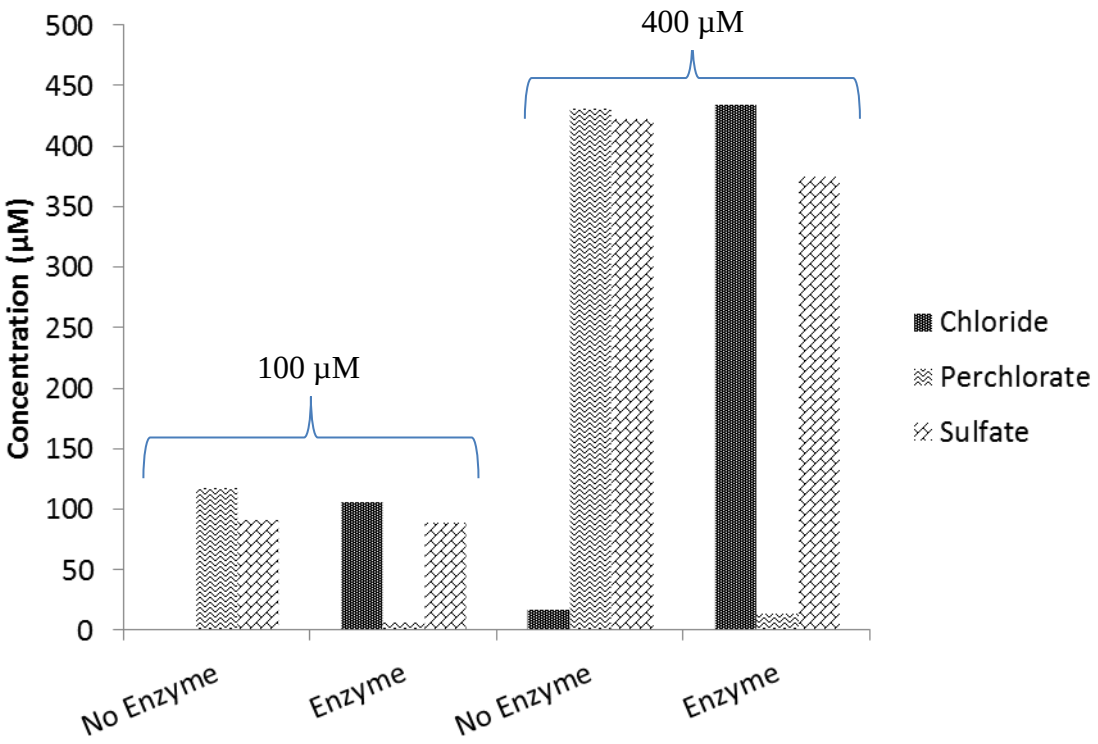

Figure 17: Competitive Anion Reduction in the Presence of Sulfate.
Sulfate did not inhibit the reduction of perchlorate nor was it reduced by the perchlorate reducing enzymes. No chlorate or chlorite peaks were observed in capillary electrophoresis analysis. All sets include 500 µM NADH. The first two sets of bars include 100 µM of perchlorate and sulfate with or without soluble protein fraction containing perchlorate-reducing enzymes. The last two sets of bars include 400 µM of perchlorate and sulfate with or without enzymes. Reaction assays were incubated with the indicated concentration of each anion and 20 µL of soluble protein fraction. The small decrease in sulfate from No Enzyme to Enzyme in 100 µM and the larger decrease in 400 µM are thought to be matrix effects associated with sulfate and perchlorate eluting at similar times. Assays were performed with one biological sample.

Nitrate was competitively reduced with perchlorate; however, the enzymes' affinity for perchlorate was much higher (Figure 18). This is consistent with the perchlorate-reducing organism of GR-1. The strain's washed cell suspension when grown on perchlorate was unable to grow on nitrate [52]. At 100 µM concentrations of perchlorate and nitrate, the anions were reduced to very low concentrations. However, at 400 µM concentrations of the anions and limiting NADH concentration, perchlorate and nitrate were reduced by 84% and 15% respectively. However, despite the competitive effects of nitrate, the formation of chlorate or chlorite was not detected on the capillary electrophoresis.

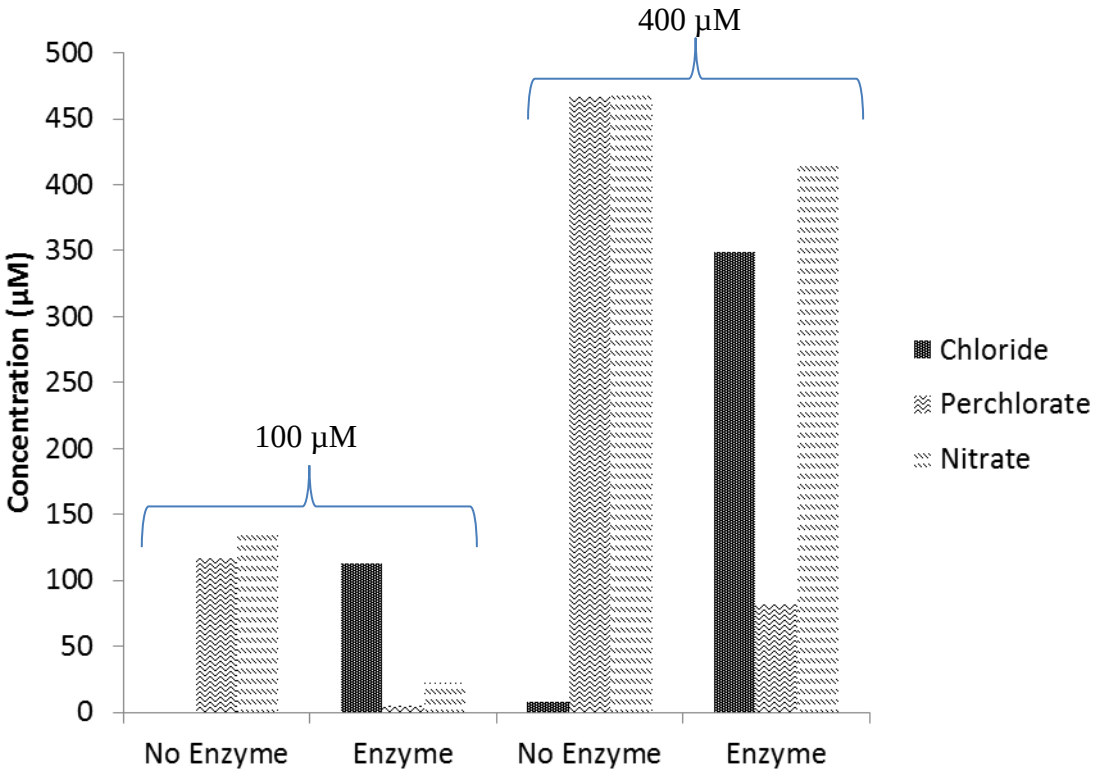

Figure 18: Competitive Anion Reduction in the Presence of Nitrate.
Nitrate is shown to compete for electron donor, NADH. However, enzymes show greater affinity for perchlorate. All sets include 500 µM NADH. The first two sets of bars include 100 µM of perchlorate and nitrate with or without enzymes. The last two sets of bars include 400 µM of perchlorate and nitrate with or without enzymes. Reaction assays were incubated with the indicated concentration of each anion and 20 µL of soluble protein fraction. Assays were performed with one biological sample.

4.3: PRODUCTION OF OmpF.

Study of the perchlorate-reducing enzymes pertains to one of the biologically important components of the perchlorate-reducing vesicles. The following sections are devoted to the development of the other biologically important component, the OmpF pore. OmpF, a diffusive porin, was purified for insertion into the synthetic cell. OmpF purification was conducted on the *E.coli* double mutant (*ΔompA ΔompC*) with an OmpF IPTG-inducible-overexpression vector [65]. Purification of OmpF relies on manipulation of the solubility of the OmpF associated peptidoglycan layer. SDS was used in elevated concentrations to insolubilize the peptidoglycan layer. The SDS had the additional benefit of solubilizing most non-membrane associated proteins. After separating the OmpF from other cellular proteins, OmpF was resolubilized using the detergent Octyl-POE. A final high-speed centrifugation resulted in the pelleting of the peptidoglycan layer. The soluble OmpF remained in the supernatant.

Some initial difficulties resulted from the induction of *E. coli* cells. This was resolved by using freshly prepared IPTG. Another problem occurred in the sonication of the cell pellet to disrupt the membranes. It is important to note the model number of the probe used in sonication here as it results in up to four times stronger disruption than a standard probe. Difference in probes resulted in a threefold difference in final OmpF concentration.

Purification of OmpF resulted in the monomer unit of OmpF upon heating, corresponding closely with the 37kDa published size of OmpF [65] (Figure 19). Note the dilutions decrease from Spin 1, Spin 2 and OmpF. Spin 1 was diluted with larger volumes of buffer. However, bands on the gel are very dark signifying a large amount of protein. Spin 2 also has a significant amount of protein in each band. This corresponds to a significant loss of OmpF with each spin despite the use of the insoluble nature of the OmpF-containing peptidoglycan layer.

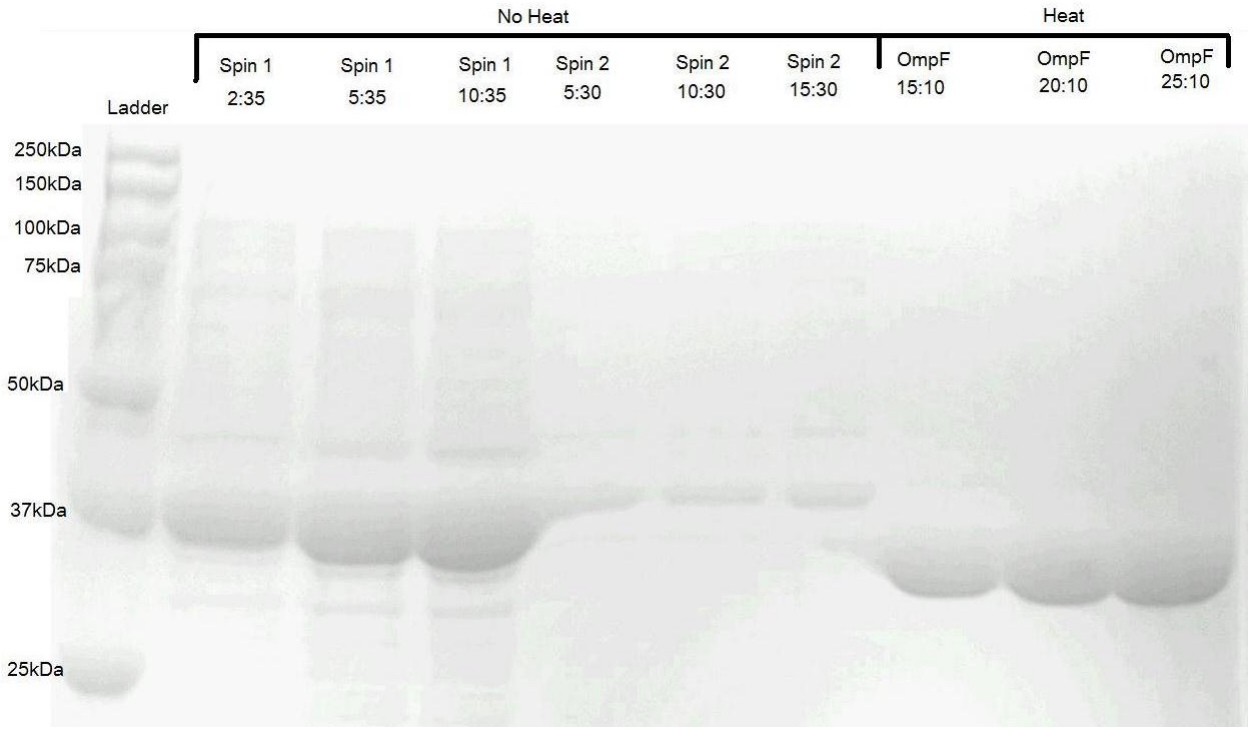

Figure 19: OmpF Purification.
The following samples were run on a 12% SDS-Page gel. Ratios indicated dilution factors for the same OmpF preparation. Spin 1 (lanes 2-4) and Spin 2 (lanes 5-7) indicate solubilized fractions of cell lysates after each centrifugation and were not heat treated. Lanes 8, 9 and 10 included the purified OmpF treated at 95°C for five minutes.

4.4: FORMATION AND ANALYSIS OF LIPID AND POLYMER VESICLES.

Having completed sections 1 through 3, the final step was to combine the biological components I had produced with lipids and synthetic polymer to form perchlorate-reducing vesicles. I also tested the vesicles' ability to protect the enzymes from protease degradation.

4.4.1 Perchlorate-Reducing Lipid Vesicles: Lipids were initially used to test the hypothesis that synthetic vesicles were capable of perchlorate degradation. Soy asolectin and cholesterol lipids were used to form vesicles with encapsulated Pcr and Cld as described in Materials and Methods. Two types of vesicles were prepared: with and without OmpF. The size and size distribution of lipid vesicles was assessed using dynamic light scattering (Figure 20). OmpF vesicles were slightly larger than No OmpF vesicles but not statistically different (n=3 P=0.254). The size distribution was determined from the polydispersivity index (PDI). For the purposes of this study, PDI values less than 0.15 were considered to represent uniform size. For lipid vesicles, the PDI for both OmpF and No OmpF vesicles were larger than 0.15. This was likely due to only extruding to a size of 400 nm. This step did not force all lipid vesicles into a uniform size. The purpose of extruding at 400 nm was to eliminate any large material. Extrusion down to 200 nm was not performed to avoid vesicle lysis and the loss of perchlorate reducing enzymes. The PDI for the two sets is significantly different (n=3 P=.018). This may be due to the presence of the detergent Octyl-POE in the OmpF vesicles.

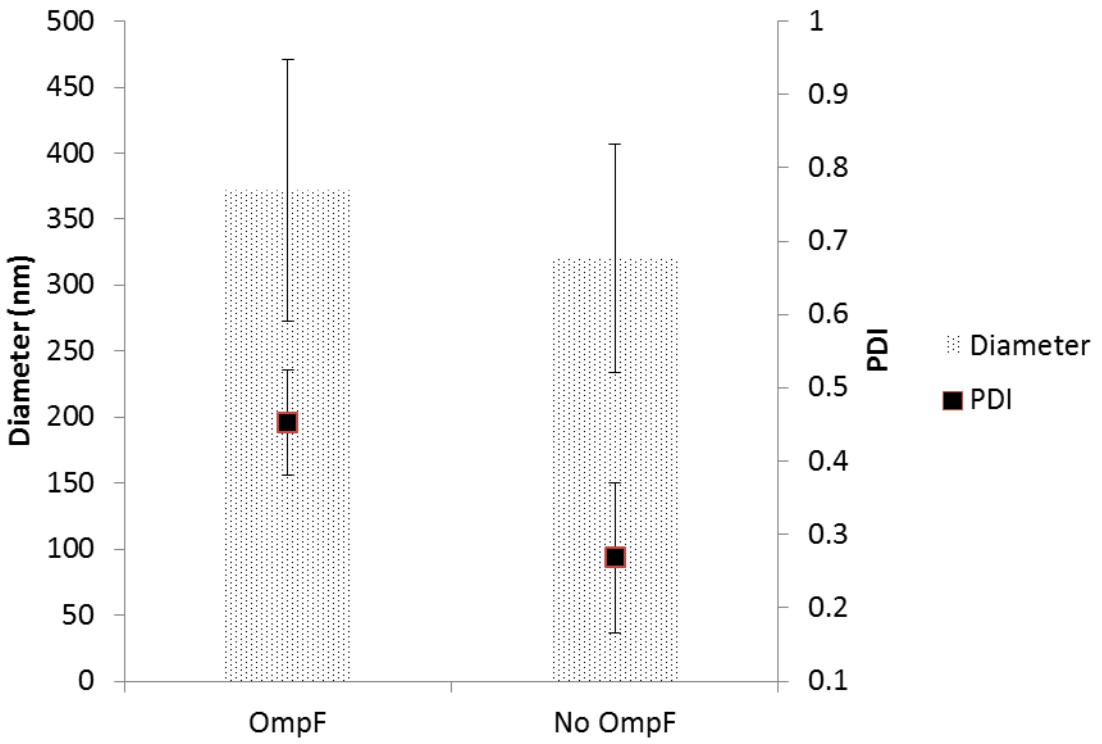

Figure 20: Size and Size Distribution of Lipid Vesicles.
The diameter and polydispersivity index (PDI) for the vesicles were recorded using dynamic light scattering (DLS). Values for size are given as average diameters. OmpF vesicles were slightly larger on average than No OmpF vesicles but not statistically different. The PDI, however, is significantly different for the two sets. The size distribution of OmpF vesicles was not as uniform as No OmpF vesicles. Error bars represent standard deviation.

Once the size of the vesicles was determined, the leakage of the vesicles was studied using the dye, carboxyfluorescein, to confirm incorporation and activity of OmpF. Vesicles were rehydrated with carboxyfluorescein and prepared as described. Once size exclusion of the vesicles was complete, fluorescence of the vesicles was measured (Figure 21). Vesicles without OmpF should be able to retain the carboxyfluorescein as there are no pores for the dye to diffuse through. No OmpF vesicles do show slightly elevated levels of fluorescence compared to OmpF vesicles. However, this difference is much smaller than values obtained in a similar experiment using polymer vesicles [64]. From the data, lipid vesicles were permeable to carboxyfluorescein. Carboxyfluorescein, with a molecular weight of 376.32 gram/mole, is a larger molecule than perchlorate which has a gram formula mass of 99.5 gram/mole. The observed permeability of

carboxyfluorescein suggests that perchlorate, a smaller molecule, can diffuse in or out of vesicles with and without OmpF.

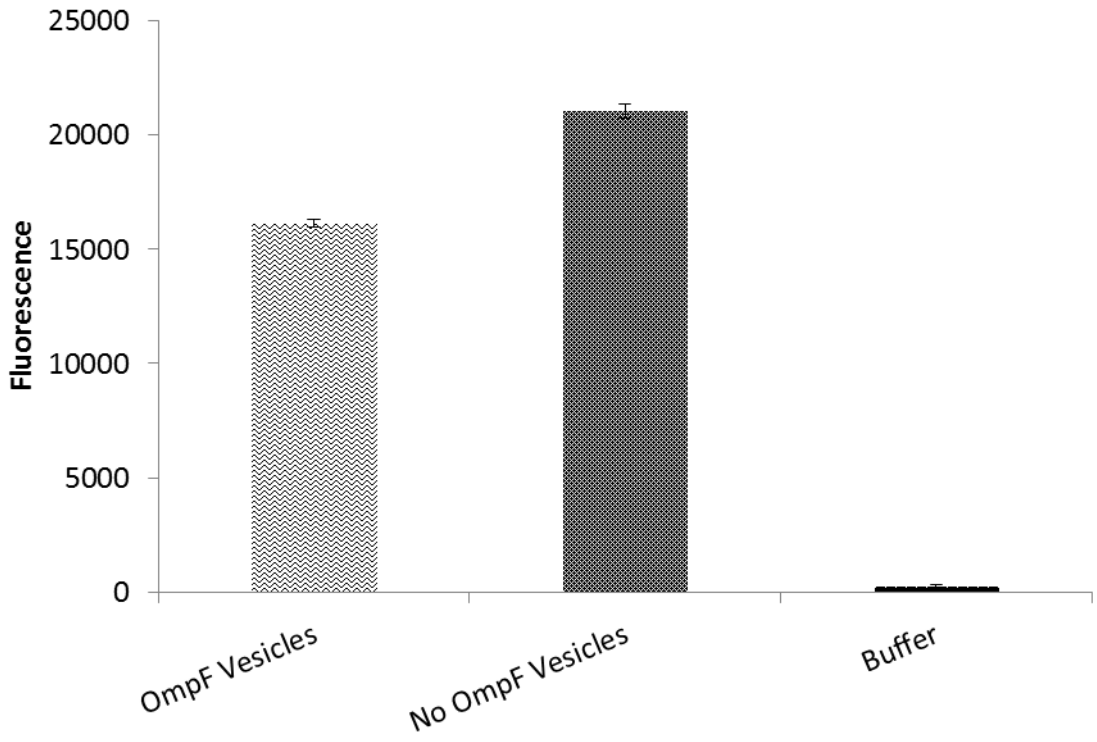

Figure 21: Retention of Fluorescence In Lipid Vesicles.
No OmpF vesicles show slightly higher fluorescence than OmpF Vesicles. Error bars represent standard deviation of six technical replicates.

After characterizing the lipid vesicles, the perchlorate-reducing activity was determined using the methyl viologen assay and 400 µL of vesicle preparation (Figure 22). All of the experiments showed significantly reduced activities compared to soluble protein fraction assay values. As detailed in the Discussion, this is likely due to the limited perchlorate-reducing volume created in the vesicles. Background activity was observed in the no perchlorate OmpF, control. This is due to minute traces of oxygen and the innate reducing power of the soluble protein fraction. However, most important was that OmpF vesicles showed statistically significant elevated activity over No OmpF vesicles (n=3 P=.012). OmpF vesicles were also

exposed to Proteinase K for one hour and 25°C to determine the lipid's ability to protect the enzymes inside the vesicles. OmpF vesicles with and without protease showed similar levels of activity (n=3 P=0.218).

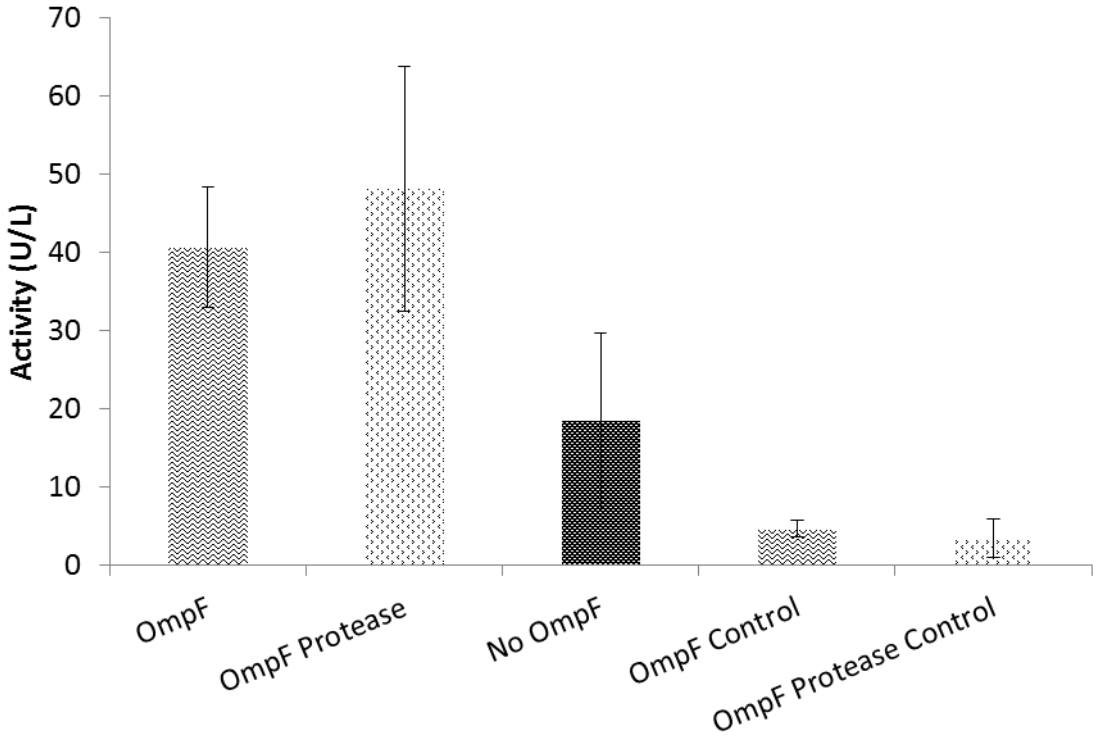

Figure 22: Perchlorate-Reducing Lipid Vesicles.
Perchlorate reduction was observed in the lipid vesicles. OmpF vesicles were capable of degrading more perchlorate than No OmpF and OmpF Control Vesicles. OmpF Protease vesicles maintain their ability to degrade perchlorate in the presence of protease. Methyl viologen assays were performed on biological triplicates. Error bars represent standard deviation.

4.4.2 Perchlorate-Reducing Polymer Vesicles: Lipid vesicles were used for proof of concept as the polymer material was in short supply but interpretation was complicated by their high permeability to carboxyfluorescein. Once the lipid vesicles were shown to reduce perchlorate, ABA polymer was used to create vesicles. An additional control, vesicles without OmpF but with detergent, was included. The detergent was hypothesized to aid in the insertion of *A. oryzae* native porins that could increase transport and thus perchlorate-reducing activity. Three different types of vesicles were prepared: 1) OmpF vesicles with the detergent Octyl-POE, 2) No OmpF vesicles with the detergent, and 3) No OmpF without detergent. The polymer vesicles were analyzed for their size and size distribution using dynamic light scattering. As shown in Figure 23, the sizes and PDIs for polymer vesicles were much smaller than lipid vesicles despite similar preparation methods. OmpF and No OmpF polymer vesicles formed similar sized vesicles (n=3 P=0.239) with similar polydispersivity indices (n=3 P=0.372). The PDI for the vesicles were within acceptable limits signifying that vesicles were uniform in size. However, the No OmpF No Detergent vesicles had an average size and PDI significantly larger than OmpF vesicles (n=3 P=0.0025 P=0.0195), and the PDI of the No OmpF, No Detergent vesicle were slightly higher than the cut off range for acceptable uniform distribution.

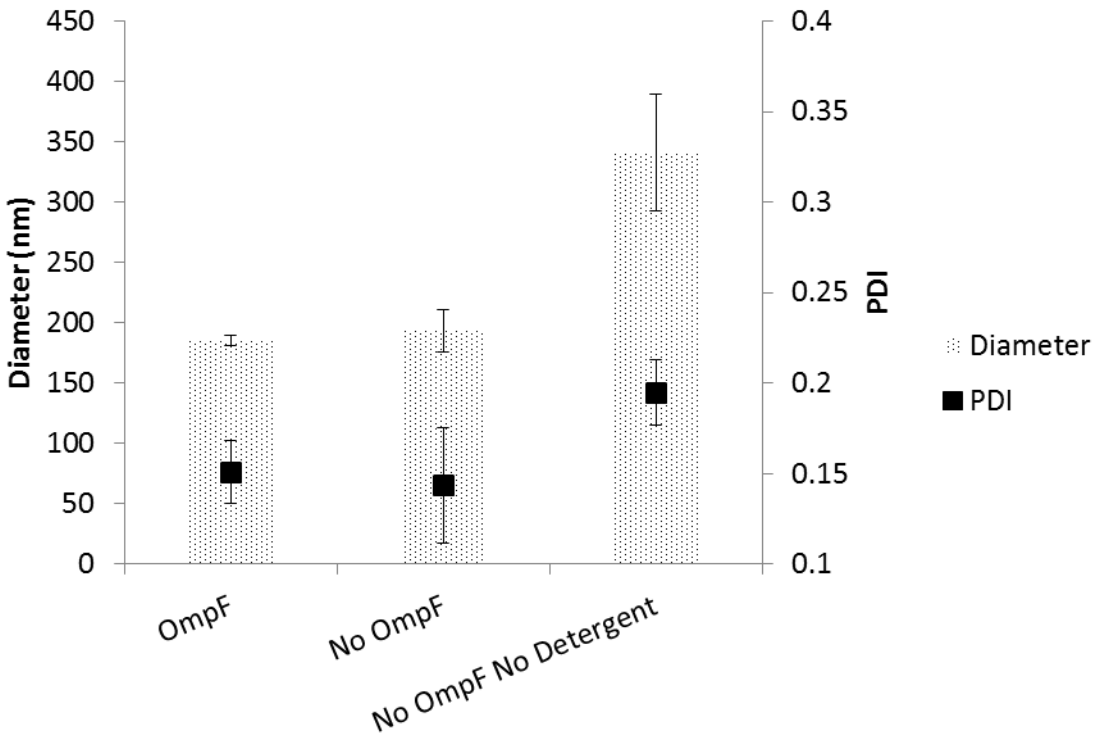

.

Figure 23: Size and Size Distribution of Polymer Vesicles.
The diameter and polydispersivity index (PDI) for the vesicles were recorded using dynamic light scattering (DLS). Vesicles containing OmpF and Detergent had a diameter and PDI that were not statistically different than No OmpF Vesicles. However, diameter and PDI between OmpF and No OmpF, No Detergent Vesicles was statistically different. Error bars represent standard deviation.

To visually determine the size and distribution of the polymer vesicles, transmission electron microscopy was used to take images of the vesicles. In Figure 24, images for OmpF, No OmpF, and No OmpF, No Detergent vesicles are shown. OmpF and No OmpF vesicles are spherical and similar in size. The diameters of the vesicles on TEM are approximately 50 nm. This is smaller than data from DLS measurements. TEM images are thought to reduce the size of vesicles due to the drying involved in sample preparation [18]. Also, the distribution of sizes of the vesicles appears to range from 20 to 50 nm. No OmpF, No Detergent form interesting polymer shapes known as worms. A plausible explanation for the formation of worms is the lack of detergent. For the purposes of the experiments, the formation of worms could result in a lower surface area to volume ratio which could affect the rate of perchlorate degradation.

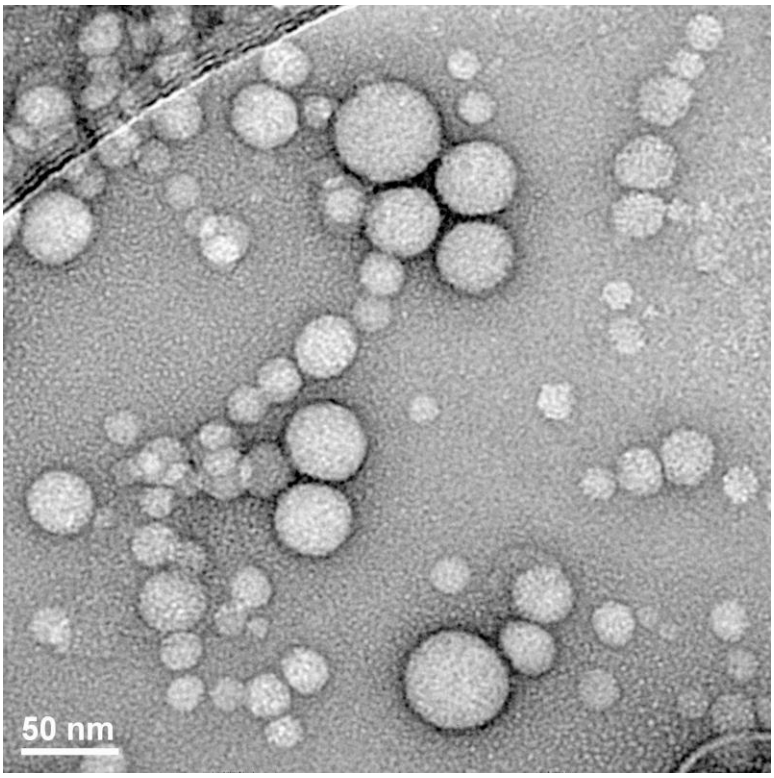

a

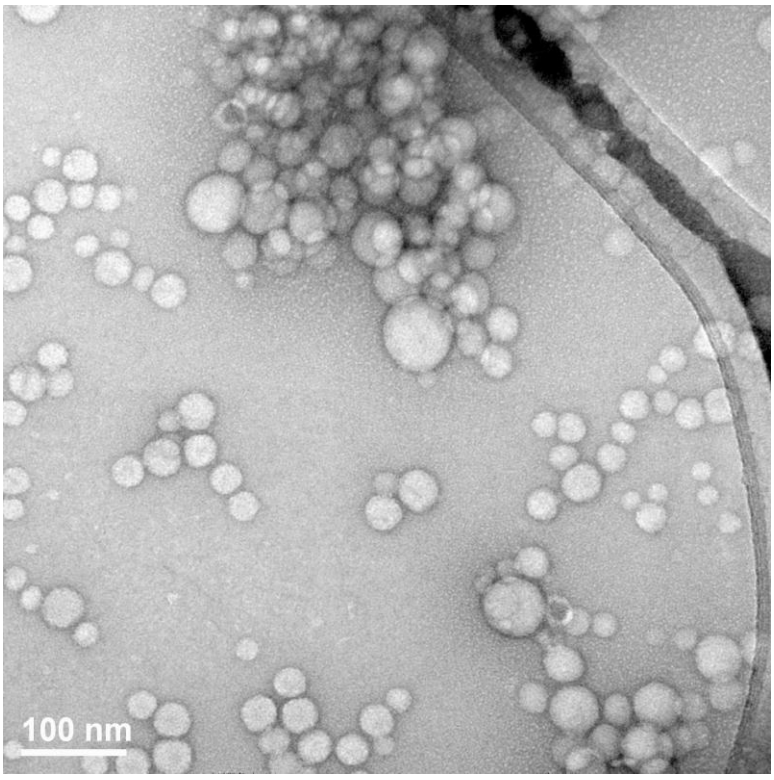

b

Figure 24 (cont.)

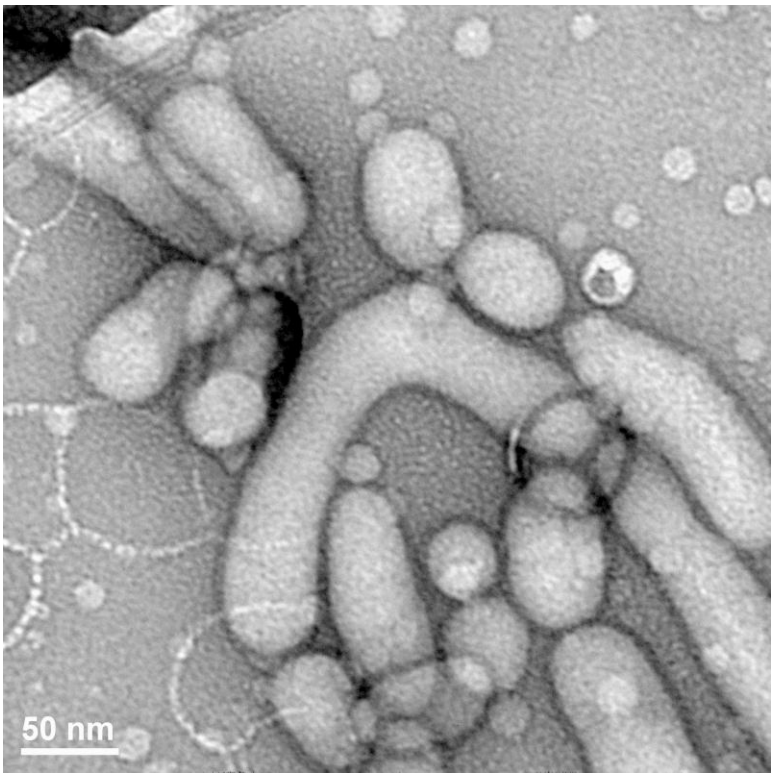

c

Figure 24: TEM Images of Polymer Vesicles.
a) OmpF vesicles are spherical and relatively uniform in size. **b)** No OmpF vesicles still have detergent in the sample that allows the formation of uniform spherical shapes. The No OmpF sample has a larger range of vesicle sizes compared to OmpF. **c)** No OmpF, No Detergent vesicles are irregular shaped forming worm-like structures.

The reducing activity of the polymer vesicles was determined using the methyl viologen assay (Figure 25). As with lipid vesicles, the polymer vesicle experiments showed significantly reduced activities compared to soluble protein fraction assay values. As detailed in the Discussion, this is likely due to the very limited perchlorate-reducing volume created in the vesicles. Background activity was observed in the OmpF control containing no perchlorate due to minute traces of oxygen and the innate reducing power of the soluble protein fraction. This background activity value was subtracted from vesicle-reducing activity. Most importantly, OmpF vesicles had statistically higher activity than No OmpF vesicles overall (n=3 P=0.0028).This trend was seen in lipids; however, lipid vesicles had lower activities compared to polymer vesicles. OmpF and No OmpF, No Detergent vesicles were also statistically different (n=3 P=0.000096). OmpF and No OmpF vesicles with detergent were also exposed to Proteinase K to determine the polymers ability to protect the enzymes inside the vesicles. A decline in the activity from protease treatment was noticed but was not statistically significant (n=3 P=0.088). This decrease could be a loss of activity resulting from the incubation at 25°C for one hour. Also, any remaining extra-vesicular enzymes could have been degraded by the protease.

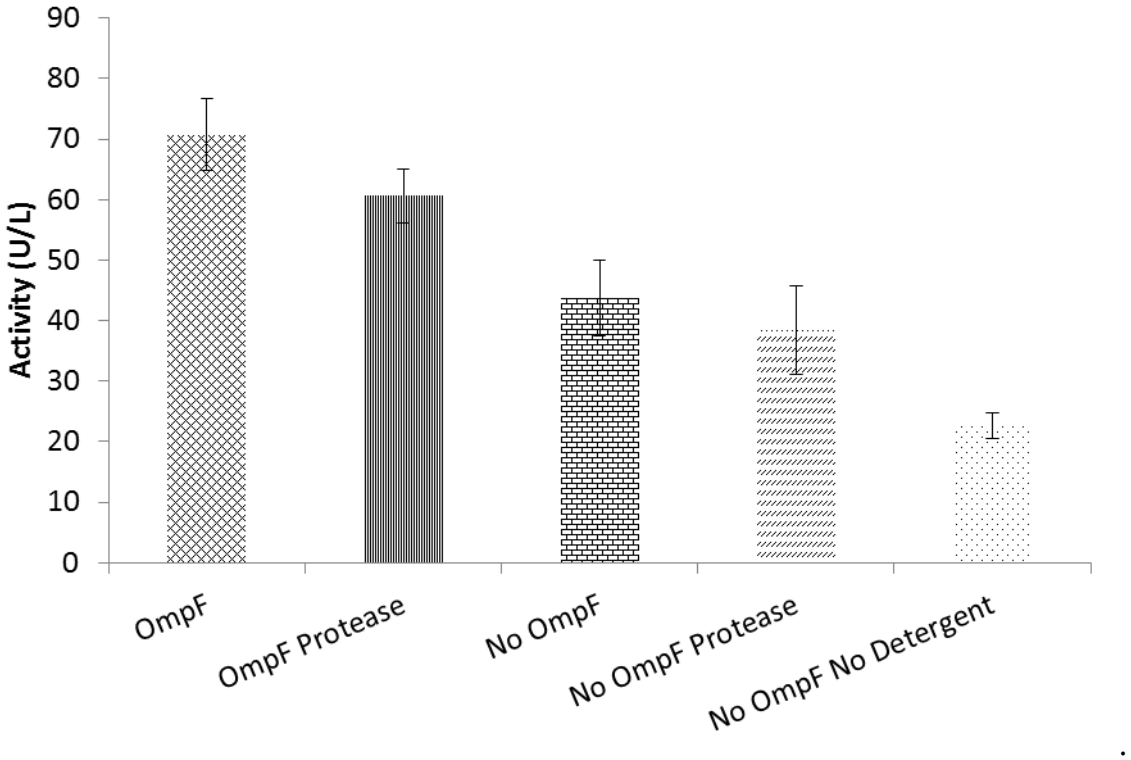

Figure 25: Reducing Activity of Polymer Vesicles.
Perchlorate reduction was observed in the polymer vesicles. OmpF vesicles were capable of degrading perchlorate at higher rates than No OmpF and No OmpF, No Detergent vesicles. OmpF vesicles maintain their ability to degrade perchlorate in the presence of protease. Background activity due to oxygen and reducing power of soluble protein fraction was measured and subtracted from activity values. Measurements were taken from biological triplicates and error bars represent standard deviation.

Observation of perchlorate-reducing activity implies perchlorate diffusion into and permeability of the vesicles. To measure the permeability of the vesicles to water, stopped-flow analysis was performed using a hyperosmotic 1 molar solution of sucrose (Figure 26). Vesicles were combined with an equal volume of osmotic solution. The rate of vesicles shrinkage was determined from light scattering. The data was fit exponentially to give the k value. The k value was used to determine permeability values from Equation 1.

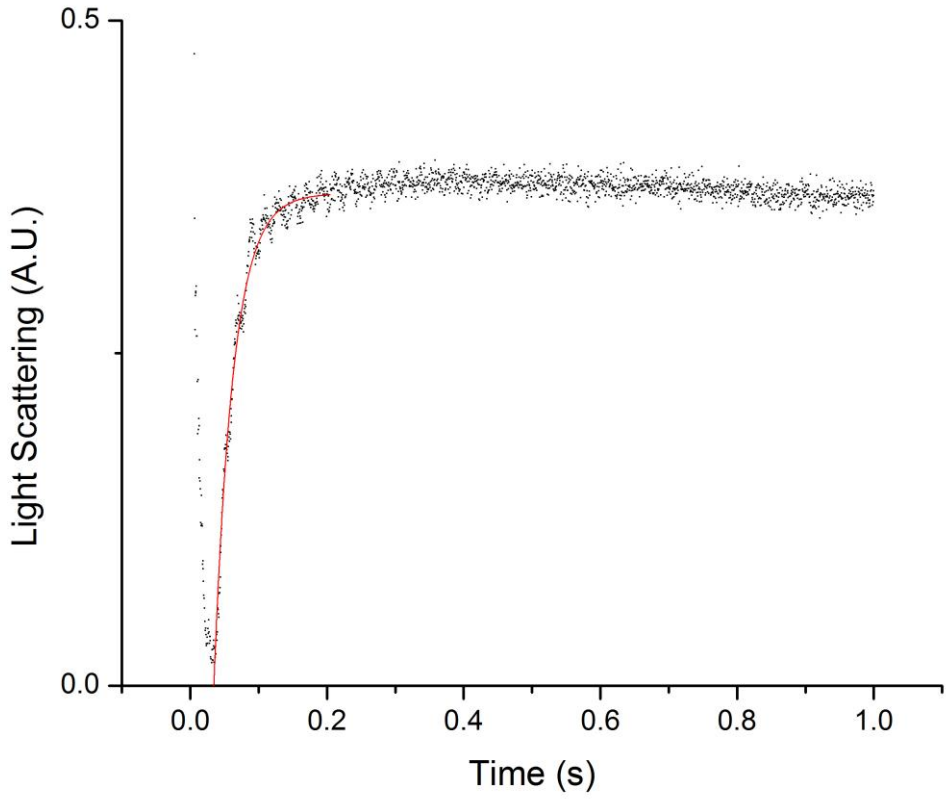

Figure 26: Typical Stopped Flow Data.
The stopped flow data registers a sharp drop in light scattering in the initial mixture of the vesicles and osmotic solution. The vesicles shrink from water leaving the vesicles causing light to scatter. The rise in scattered light is fitted exponentially and the rate of rise is determined, k.

The permeability of the vesicles was determined from using Equation 1 (Figure 27). OmpF, No OmpF and No OmpF, No Detergent vesicles were stored for approximately one month prior to measurement. An additional sample, ABA3 vesicles, was included. This sample was prepared by rehydrating in buffer with detergent. The permeability for all vesicles is very similar. This could be the result of the age of the vesicles and loss of OmpF and native porins.

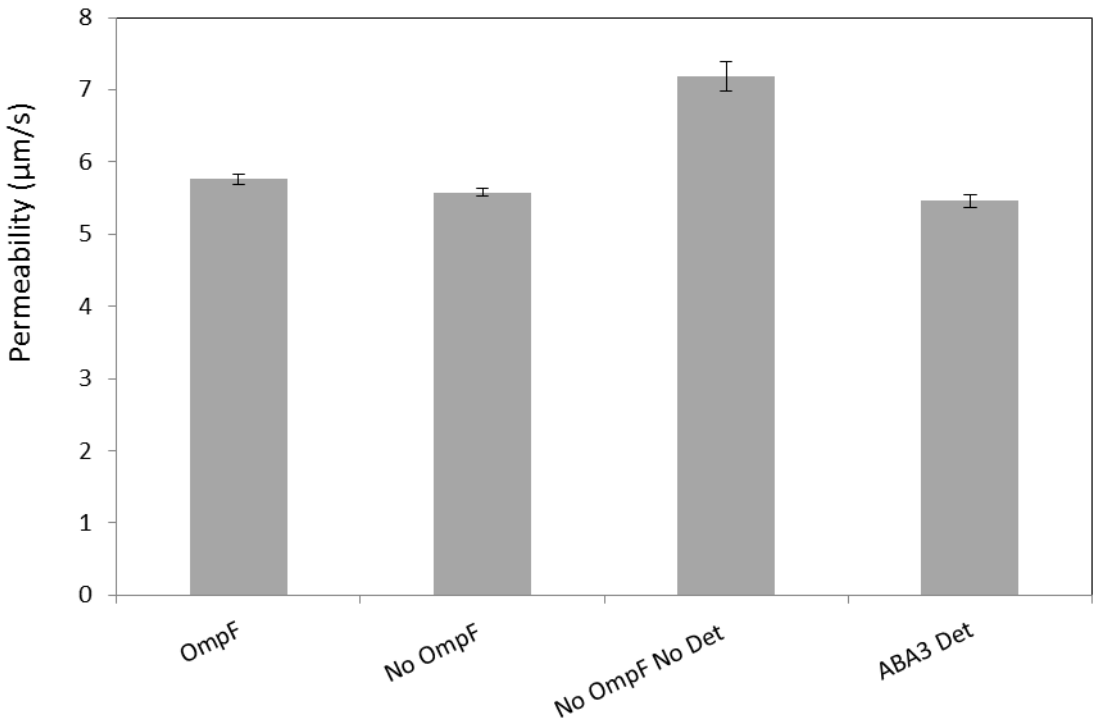

Figure 27: Permeability of Polymer Vesicles.
The permeability of the polymer vesicles to water were very similar suggesting that the number of OmpF and *A. oryzae* native porins inserted into the polymer was very low or the one-month old samples were losing permeability.

CHAPTER 5 – DISCUSSION AND CONCLUSION

This research created synthetic vesicles and assessed their ability to degrade perchlorate in a drinking water relevant aqueous environment. Perchlorate-reducing vesicles were created under laboratory conditions. The vesicle membrane was made with either natural lipids or manmade polymer. The outer membrane pore, OmpF, was inserted in the membrane material to act as a channel for perchlorate to diffuse in and out of the synthetic vesicles. Finally, partially purified perchlorate-reducing enzymes, Pcr and Cld, were encapsulated in the vesicles. This approach to perchlorate treatment uniquely combines manmade material and biological components. The approach also offers potential advantages over existing perchlorate treatment technologies. This thesis presents proof of concept for a novel treatment technology.

The unique abilities of biological enzymes, such as Pcr and Cld, to reduce targeted contaminants offer engineers a variety of tools for the treatment purposes. However, cells often have goals counter to the engineers'. Cells often require very specific conditions in which to grow. Anything that may disturb the growth of the organism such as a change in electron donor or acceptor, temperature or agitation could reduce the elimination of contaminants. By isolating and purifying the tool used for cleanup, scientists may be better able to control the cleanup process in order to achieve a specific goal. This research offers a method to accomplish those goals by allowing engineers to take biologically developed tools such as contaminant-degrading enzymes and encapsulate the enzymes in a synthetic vesicle. Once formed, the vesicles are introduced into the targeted contaminant area. Contaminants diffuse or are transported into the synthetic vesicles where enzymes turn the contaminant into an innocuous substance. The unique approach of combining synthetic and biological materials for the elimination of a contaminant has been successfully shown for perchlorate in this thesis.

This unique approach may have advantages over current treatment technologies for drinking water applications. For perchlorate, many of the drinking water treatment technologies have limitations associated with removal of concentrated waste, slow kinetics and unreliability.

For separation technologies such as GAC, IC and membranes, the drawback with these technologies is the associated concentrated wastes. The synthetic vesicle technology circumvents this problem by degrading perchlorate into chloride. Perchlorate-degrading technologies such as chemical and biological reduction are limited by the use of heavy metals, slow kinetics, and fastidious environmental conditions respectively. While the enzymes in synthetic vesicles contain heavy metals, the metals are in the interior of the vesicles which are easily contained by membranes. The kinetics of the vesicles at this time are slow; however, optimization of the diffusion of perchlorate into the vesicles and creating a column with a high concentration of these vesicles should improve the kinetics of perchlorate degradation. Finally, since the enzymes associated with perchlorate degradation are no longer in living cells, many of the environmental conditions required for biological reduction, such as absence of oxygen and nitrate, are no longer necessary.

Despite the potential advantages this treatment technology has over current treatment technologies, this is a novel approach to water treatment. As such, significant research lies ahead before this system could be applied. This thesis has made progress on four key areas: (I) stabilizing the perchlorate-reducing enzymes in water treatment relevant aqueous conditions, (II) understanding the enzymes' susceptibility to simulated microbial degradation using proteases, (III) studying the competitive effects of similar anions and (IV) exploring potential reasons for the limited perchlorate degradation rates seen in vesicles. However, for each of these items, additional work needs to be conducted to answer remaining concerns.

I) Stabilization of perchlorate-reducing enzymes.

Preparation of the soluble protein fraction, containing the perchlorate-reducing enzymes, Pcr and Cld, in aerobic environments did not affect the activities of the enzymes compared to anaerobic preparation. Also, 10% glycerol was found to extend the enzymes half-life significantly over a two-day period. Previous research demonstrated enzymes' losing activity

with exposure to oxygen, with stabilization by the addition of 10% glycerol [51], while other research demonstrated that the deterioration of enzymatic activity occurred irrespective of oxygen presence [59].The difference in the effects of oxygen exposure and the glycerol stabilizing effect is likely caused by the use of different bacteria. Stabilizing the enzymes over time was essential in the formation of vesicles. Loss of significant portions of enzymatic activity over three days could result in vesicles with no functioning enzymes. Also, the application of the vesicles in the treatment of perchlorate-contaminated drinking water requires functionality in the order of months. For application in drinking water treatment, further research into increasing the half-life of the enzymes must be conducted. Experiments could include storing enzymes in perchlorate and electron donor to protect functional sites.

II) Determination of the Effects of Protease Inhibitors and Proteinase K.

Surprisingly, addition of a broad-spectrum protease inhibitor resulted in decreased enzyme activity. One possible explanation includes the potential protective nature of native proteases to perchlorate-reducing enzymes. The native proteases may be responsible for inactivation of Pcr and Cld degrading enzymes. To answer this question, future experiments could examine the possibility of an *Azospira oryzae* native protease responsible for perchlorate-reducing enzyme protection. Also unexpected, treatment with the Proteinase K did not result in complete inactivation of the enzymes. This is likely due to the use of protease concentrations and exposure time less than recommended. The enzymes' susceptibility to protease should be examined using higher protease concentrations, extended incubation times and varying incubation temperatures.

III) Competition of Similar Anions.

The enzymes responsible for perchlorate reduction were tested for reductive abilities against sulfate and nitrate due to these anions' common inhibitory effect on current perchlorate

treatment technologies. The soluble protein fraction was able to reduce perchlorate and nitrate but not sulfate. The soluble protein fraction's ability to reduce nitrate even at low rates is not desired. This is due to the presence of nitrate in drinking waters generally at concentrations in the ppm range whereas perchlorate concentrations are less than 100 ppb [78]. The competitive nature of the enzymatic enzymes for perchlorate and nitrate was assessed. Although both nitrate and perchlorate were reduced in environments where the anions concentrations were similar, the enzymes in the soluble protein fraction had greater affinity for perchlorate. Significant additional work should be conducted to verify perchlorate reduction in the presence of excess nitrate. These experiments should be conducted with anion ratios similar to those found in drinking water systems. Depending on these results, perchlorate-reducing enzymes from *Azospria oryzae* may not be an ideal candidate for use in synthetic perchlorate-reducing vesicles. Other bacteria unable to grow on nitrate may present a better alternative. Additional anions such as selenate, borate, iodate, and carbonate should also be assessed for activity with perchlorate reductase and chlorite dismutase. It is interesting to note that the chlorate and chlorite intermediates did not form suggesting that once the enzyme, Pcr, encounters perchlorate; it sequentially reduces perchlorate to chlorite without releasing the anion in the intermediate step. Chlorite, with its reduction having been previously shown to be independent of an electron donor [62], did not accumulate in the experiments.

IV) Exploration of the Reasons For Limited Perchlorate-Degradation

The results of this thesis suggest that synthetic cells are capable of reducing perchlorate into chloride. The main issue remaining is the optimization of these perchlorate-reducing vesicles. The activity of the vesicles was significantly reduced compared to enzyme lysates. Possible explanations include inefficient enzyme encapsulation and limited perchlorate diffusion. As an initial assessment, the theoretical consequences of both potential limitations were calculated as detailed in Appendix C.

The first set of equations examines the volume of vesicles when using 12 mg of polymer. As seen in the calculations, volume of the vesicles could be a limiting factor as theoretical calculations put perchlorate-reducing activity at a 2 fold higher rate, 149 Units/Liter, than obtained experimentally. This value is very similar to experimental values and could explain the

lower perchlorate-reducing vesicle activity compared to the soluble protein fraction. The small discrepancy between the volume encapsulation calculations and experimental values could be inefficient or preferential encapsulation of enzymes. Also, the theoretical calculations performed may fail to take into account several factors including lost polymer and release of enzymes during extrusion and size exclusion. Heterologous overexpression of both perchlorate reductase and chlorite dismutase would assure a higher concentration of perchlorate-reducing enzymes are encapsulated and provide additional data on perchlorate-reducing reaction rates.

In additional to volume encapsulation calculations, perchlorate diffusion through OmpF into polymer vesicles was calculated using Fick's Law and surface area calculations. The activity that could result from perchlorate diffusion is 4,910,000 U/L. This calculated activity demonstrates that transport of perchlorate into the vesicles does not seem to be the limiting factor. Even with hindered diffusion, which could reduce flux by 99%, the rate at which perchlorate enters the vesicles is sufficient to maintain higher levels of activity than were observed by 5 orders of magnitude. Volume limitation is therefore most likely to restrict the level of enzyme activity seen in my research.

Optimizing these synthetic vesicles to increase perchlorate reduction rates could eliminate a major hurdle in the application of this treatment technology. The use of these vesicles also presents many advantages over current treatment technologies as outlined previously. In this thesis, I have demonstrated the synthetic vesicles abilities' to reduce perchlorate in relevant drinking water treatment conditions. The vesicles are able to protect the encapsulated enzymes from degradation associated with proteases. This work has also created the framework for producing vesicles capable of targeting other contaminants by selecting biological contaminant-specific degrading enzymes.

REFERENCES

1. Report: More than One Out of Three U.S. Counties Face Water Shortages Due to Climate Change. In 2010.
2. Greer, M. A.; Goodman, G.; Pleus, R. C.; Greer, S. E., Health effects assessment for environmental perchlorate contamination: the dose response for inhibition of thyroidal radioiodine uptake in humans. *Environ Health Perspect* **2002,** *110*, (9), 927-37.
3. Motzer, W. E., Perchlorate: Problems, detection, and solutions. *Environ Forensics* **2001,** *2*, (4), 301-311.
4. Waller, A. S.; Cox, E. E.; Edwards, E. A., Perchlorate-reducing microorganisms isolated from contaminated sites. *Environmental microbiology* **2004,** *6*, (5), 517-27.
5. Godley, A. F.; Stanbury, J. B., Preliminary experience in the treatment of hyperthyroidism with potassium perchlorate. *The Journal of clinical endocrinology and metabolism* **1954,** *14*, (1), 70-8.
6. Crump, C.; Michaud, P.; Téllez, R.; Reyes, C.; Gonzalez, G.; Montgomery, E. L.; Crump, K. S.; Lobo, G.; Becerra, C.; Gibbs, J. P., Does Perchlorate in Drinking Water Affect Thyroid Function in Newborns or School-Age Children? *Journal of Occupational and Environmental Medicine* **2000,** *42*, (6), 603-612.
7. Levy, O.; Dai, G.; Riedel, C.; Ginter, C. S.; Paul, E. M.; Lebowitz, A. N.; Carrasco, N., Characterization of the thyroid Na+/I- symporter with an anti-COOH terminus antibody. *Proceedings of the National Academy of Sciences of the United States of America* **1997,** *94*, (11), 5568-73.
8. Tonacchera, M.; Pinchera, A.; Dimida, A.; Ferrarini, E.; Agretti, P.; Vitti, P.; Santini, F.; Crump, K.; Gibbs, J., Relative potencies and additivity of perchlorate, thiocyanate, nitrate, and iodide on the inhibition of radioactive iodide uptake by the human sodium iodide symporter. *thyroid* **2004,** *14*, (12), 1012-9.
9. Cooper, D. S., Subclinical Hypothyroidism. *JAMA: The Journal of the American Medical Association* **1987,** *258*, (2), 246-247.
10. Lamm, S. H.; Braverman, L. E.; Li, F. X.; Richman, K.; Pino, S.; Howearth, G., Thyroid health status of ammonium perchlorate workers: a cross-sectional occupational health study. *Journal of occupational and environmental medicine / American College of Occupational and Environmental Medicine* **1999,** *41*, (4), 248-60.
11. Perchlorate: A System to Track Sampling and Cleanup Results is Needed. In United States Government Accountability Office, 2005.
12. Perchlorate Environmental Contamination: Toxicological Review and Risk Characterization. In Agency, U. S. E. P., Ed. 2002.
13. Drinking Water: Preliminary Regulatory Determination on Perchlorate. In Agency, U. S. E. P., Ed. Federal Register, 2008; Vol. 73, pp 60262-60282.
14. EPA Seeks Advice on Perchlorate in Drinking Water - Agency Issues Interim Health Advisory. In United States Environmental Protection Agency: 2009.
15. EPA Seeks Comments on its Reevaluation of the Chemical Perchlorate. In United States Environmental Protection Agency: 2009.
16. Zewdie, T.; Smith, C. M.; Hutcheson, M.; West, C. R., Basis of the Massachusetts reference dose and drinking water standard for perchlorate. *Environ Health Perspect* **2010,** *118*, (1), 42-8.
17. Nardin, C.; Hirt, T.; Leukel, J.; Meier, W., Polymerized ABA Triblock Copolymer Vesicles. *Langmuir* **2000,** *16*, (3), 1035-1041.
18. Kumar, M.; Grzelakowski, M.; Zilles, J.; Clark, M.; Meier, W., Highly permeable polymeric membranes based on the incorporation of the functional water channel protein Aquaporin Z. *Proceedings of the National Academy of Sciences of the United States of America* **2007,** *104*, (52), 20719-24.

19. Choi, H. J.; Montemagno, C. D., Artificial organelle: ATP synthesis from cellular mimetic polymersomes. *Nano letters* **2005,** *5*, (12), 2538-42.
20. Discher, D. E.; Ahmed, F., Polymersomes. *Annual review of biomedical engineering* **2006,** *8*, 323-41.
21. Discher, D. E.; Eisenberg, A., Polymer vesicles. *Science* **2002,** *297*, (5583), 967-73.
22. Flores, C. M. The Stability of Phospholipid and Biomimetic Polymer Vesicles. University of Illinois, Urbana, IL, 2012.
23. Brown, J. C.; Anderson, R. D.; Min, J. H.; Boulos, L.; Prasifka, D.; Juby, G. J. G., Fixed bed biological treatment of perchlorate-contaminated drinking water. *Journal American Water Works Association* **2005,** *97*, (9), 70-81.
24. Vidali, M., Bioremediation. An overview. *Pure Appl Chem* **2001,** *73*, (7), 1163-1172.
25. Drinking Water: Regulatory Determination on Perchlorate. In United States Environmental Protection Agency: Federal Register, 2011; Vol. 76, pp 7762-7767.
26. Perchlorate Treatment Technology Update. In United States Environmental Protection Agency: 2005.
27. Srinivasan, R.; Sorial, G. A., Treatment of perchlorate in drinking water: A critical review. *Separation and Purification Technology* **2009,** *69*, (1), 7-21.
28. Parette, R.; Cannon, F. S., The removal of perchlorate from groundwater by activated carbon tailored with cationic surfactants. *Water research* **2005,** *39*, (16), 4020-4028.
29. Na, C. Z.; Cannon, F. S.; Hagerup, B., Perchlorate removal via iron-preloaded GAC and borohydride regeneration. *Journal American Water Works Association* **2002,** *94*, (11), 90-102.
30. Chen, W. F.; Cannon, F. S.; Rangel-Mendez, J. R., Ammonia-tailoring of GAC to enhance perchlorate removal. I: Characterization of NH3 thermally tailored GACs. *Carbon* **2005,** *43*, (3), 573-580.
31. Chen, W. F.; Cannon, F. S.; Rangel-Mendez, J. R., Ammonia-tailoring of GAC to enhance perchlorate removal. II: Perchlorate adsorption. *Carbon* **2005,** *43*, (3), 581-590.
32. Yoon, J.; Amy, G.; Chung, J.; Sohn, J.; Yoon, Y., Removal of toxic ions (chromate, arsenate, and perchlorate) using reverse osmosis, nanofiltration, and ultrafiltration membranes. *Chemosphere* **2009,** *77*, (2), 228-235.
33. Huq, H. P.; Yang, J.-S.; Yang, J.-W., Removal of perchlorate from groundwater by the polyelectolyte-enhanced ultrafiltration process. *Desalination* **2007,** *204*, (1–3), 335-343.
34. Roach, J. D.; Tush, D., Equilibrium dialysis and ultrafiltration investigations of perchlorate removal from aqueous solution using poly(diallyldimethylammonium) chloride. *Water research* **2008,** *42*, (4–5), 1204-1210.
35. Yoon, Y.; Amy, G.; Cho, J.; Her, N.; Pellegrino, J., Transport of perchlorate (ClO4−) through NF and UF membranes. *Desalination* **2002,** *147*, (1–3), 11-17.
36. Yoon, Y.; Amy, G.; Yoon, J., Effect of pH and conductivity on hindered diffusion of perchlorate ions during transport through negatively charged nanofiltration and ultrafiltration membranes. *Desalination* **2005,** *177*, (1–3), 217-227.
37. Gu, B.; Ku, Y.-K.; Brown, G. M., Treatment of Perchlorate-Contaminated Groundwater Using Highly Selective, Regenerable Ion-Exchange Technology: A Pilot-Scale Demonstration. *Remediation Journal* **2002,** *12*, (2), 51-68.
38. Gu, B.; Brown, G. M.; Maya, L.; Lance, M. J.; Moyer, B. A., Regeneration of Perchlorate (ClO4-)-Loaded Anion Exchange Resins by a Novel Tetrachloroferrate (FeCl4-) Displacement Technique. *Environmental science & technology* **2001,** *35*, (16), 3363-3368.
39. Ion-exchange system removes perchlorate. *Membrane Technology* **2006,** *2006*, (4), 3-4.
40. Pakzadeh, B.; Batista, J. R., Impacts of Cocontaminants on the Performances of Perchlorate and Nitrate Specialty Ion-Exchange Resins. *Industrial & Engineering Chemistry Research* **2011,** *50*, (12), 7484-7493.

41. Gu, B.; Dong, W.; Brown, G. M.; Cole, D. R., Complete Degradation of Perchlorate in Ferric Chloride and Hydrochloric Acid under Controlled Temperature and Pressure. *Environmental science & technology* **2003,** *37*, (10), 2291-2295.
42. Hurley, K. D.; Shapley, J. R., Efficient heterogeneous catalytic reduction of perchlorate in water. *Environmental science & technology* **2007,** *41*, (6), 2044-9.
43. Abu-Omar, M. M.; Espenson, J. H., Facile Abstraction of Successive Oxygen Atoms from Perchlorate Ions by Methylrhenium Dioxide. *Inorganic chemistry* **1995,** *34*, (25), 6239-6240.
44. Abu-Omar, M. M.; Appelman, E. H.; Espenson, J. H., Oxygen-Transfer Reactions of Methylrhenium Oxides. *Inorganic chemistry* **1996,** *35*, (26), 7751-7757.
45. Wang, D. M.; Shah, S. I.; Chen, J. G.; Huang, C. P., Catalytic reduction of perchlorate by H2 gas in dilute aqueous solutions. *Separation and Purification Technology* **2008,** *60*, (1), 14-21.
46. Moore, A. M.; De Leon, C. H.; Young, T. M., Rate and extent of aqueous perchlorate removal by iron surfaces. *Environmental science & technology* **2003,** *37*, (14), 3189-98.
47. Láng, G. G.; Horányi, G., Some interesting aspects of the catalytic and electrocatalytic reduction of perchlorate ions. *Journal of Electroanalytical Chemistry* **2003,** *552*, (0), 197-211.
48. Moore, A. M.; Young, T. M., Chloride Interactions with Iron Surfaces: Implications for Perchlorate and Nitrate Remediation Using Permeable Reactive Barriers. *Journal of Environmental Engineering* **2005,** *131*, (6), 924.
49. Colom, F.; Gonzalez-Tejera, M. J., Reduction of Perchlorate Ion on Ruthenium Electrodes in Aqueous-Solutions. *Journal of Electroanalytical Chemistry* **1985,** *190*, (1-2), 243-255.
50. Coates, J. D.; Michaelidou, U.; Bruce, R. A.; O'Connor, S. M.; Crespi, J. N.; Achenbach, L. A., Ubiquity and diversity of dissimilatory (per)chlorate-reducing bacteria. *Appl Environ Microbiol* **1999,** *65*, (12), 5234-41.
51. Rikken, G. B.; Kroon, A. G. M.; vanGinkel, C. G., Transformation of (per)chlorate into chloride by a newly isolated bacterium: Reduction and dismutation. *Applied microbiology and biotechnology* **1996,** *45*, (3), 420-426.
52. Kengen, S. W.; Rikken, G. B.; Hagen, W. R.; van Ginkel, C. G.; Stams, A. J., Purification and characterization of (per)chlorate reductase from the chlorate-respiring strain GR-1. *Journal of bacteriology* **1999,** *181*, (21), 6706-11.
53. Hatzinger, P. B.; Whittier, M. C.; Arkins, M. D.; Bryan, C. W.; Guarini, W. J., In-Situ and Ex-Situ Bioremediation Options for Treating Perchlorate in Groundwater. *Remediation Journal* **2002,** *12*, (2), 69-86.
54. Holdren, G. C.; Kelly, K.; Weghorst, P., Evaluation of potential impacts of perchlorate in the Colorado River on the Salton Sea, California The Salton Sea Centennial Symposium. In Hurlbert, S. H., Ed. Springer Netherlands: 2008; Vol. 201, pp 173-179.
55. Achenbach, L. A.; Michaelidou, U.; Bruce, R. A.; Fryman, J.; Coates, J. D., *Dechloromonas agitata* gen. nov., sp. nov. and *Dechlorosoma suillum* gen. nov., sp. nov., two novel environmentally dominant (per)chlorate-reducing bacteria and their phylogenetic position. *Int J Syst Evol Microbiol* **2001,** *51*, (Pt 2), 527-33.
56. Oosterkamp, M. J.; Mehboob, F.; Schraa, G.; Plugge, C. M.; Stams, A. J., Nitrate and (per)chlorate reduction pathways in (per)chlorate-reducing bacteria. *Biochem Soc Trans* **2011,** *39*, (1), 230-5.
57. Moura, J. J.; Brondino, C. D.; Trincao, J.; Romao, M. J., Mo and W bis-MGD enzymes: nitrate reductases and formate dehydrogenases. *Journal of biological inorganic chemistry : JBIC : a publication of the Society of Biological Inorganic Chemistry* **2004,** *9*, (7), 791-9.
58. Wolterink, A.; Kim, S.; Muusse, M.; Kim, I. S.; Roholl, P. J.; van Ginkel, C. G.; Stams, A. J.; Kengen, S. W., *Dechloromonas hortensis* sp. nov. and strain ASK-1, two novel (per)chlorate-reducing bacteria, and taxonomic description of strain GR-1. *Int J Syst Evol Microbiol* **2005,** *55*, (Pt 5), 2063-8.

59. Sexton, J. M. Subcloning and partial purification of perchlorate reductase from *Dechloromonas aromatica* rcb. 2007.
60. Coates, J. D.; Achenbach, L. A., Microbial perchlorate reduction: rocket-fueled metabolism. *Nature reviews. Microbiology* **2004,** *2*, (7), 569-80.
61. Mehboob, F.; Wolterink, A. F.; Vermeulen, A. J.; Jiang, B.; Hagedoorn, P. L.; Stams, A. J.; Kengen, S. W., Purification and characterization of a chlorite dismutase from *Pseudomonas chloritidismutans*. *FEMS microbiology letters* **2009,** *293*, (1), 115-21.
62. van Ginkel, C. G.; Rikken, G. B.; Kroon, A. G. M.; Kengen, S. W. M., Purification and characterization of chlorite dismutase: a novel oxygen-generating enzyme. *Archives of Microbiology* **1996,** *166*, (5), 321-326.
63. Streit, B. R.; DuBois, J. L., Chemical and steady-state kinetic analyses of a heterologously expressed heme dependent chlorite dismutase. *Biochemistry* **2008,** *47*, (19), 5271-80.
64. Poust, S. K. Engineered Vesicles for Perchlorate Degradation. University of Illinois, 2010.
65. Prilipov, A.; Phale, P. S.; Van Gelder, P.; Rosenbusch, J. P.; Koebnik, R., Coupling site-directed mutagenesis with high-level expression: large scale production of mutant porins from E. coli. *FEMS microbiology letters* **1998,** *163*, (1), 65-72.
66. Grzelakowski, M.; Onaca, O.; Rigler, P.; Kumar, M.; Meier, W., Immobilized protein-polymer nanoreactors. *Small* **2009,** *5*, (22), 2545-8.
67. Lugtenberg, B.; Meijers, J.; Peters, R.; van der Hoek, P.; van Alphen, L., Electrophoretic resolution of the 'major outer membrane protein' of *Escherichia coli* K12 into four bands. *FEBS Letters* **1975,** *58*, (1-2), 254-258.
68. Tanner, R. S.; McInerney, M. J.; Nagle, D. P., Formate auxotroph of *Methanobacterium thermoautotrophicum* Marburg. *Journal of bacteriology* **1989,** *171*, (12), 6534-6538.
69. Heinnickel, M.; Smith, S. C.; Koo, J.; O'Connor, S. M.; Coates, J. D., A bioassay for the detection of perchlorate in the ppb range. *Environmental science & technology* **2011,** *45*, (7), 2958-64.
70. Ellington, J. J.; Wolfe, N. L.; Garrison, A. W.; Evans, J. J.; Avants, J. K.; Teng, Q., Determination of Perchlorate in Tobacco Plants and Tobacco Products. *Environmental science & technology* **2001,** *35*, (15), 3213-3218.
71. Chaudhuri, S. K.; O'Connor, S. M.; Gustavson, R. L.; Achenbach, L. A.; Coates, J. D., Environmental factors that control microbial perchlorate reduction. *Applied and Environmental Microbiology* **2002,** *68*, (9), 4425-4430.
72. Thrash, J. C.; Van Trump, J. I.; Weber, K. A.; Miller, E.; Achenbach, L. A.; Coates, J. D., Electrochemical stimulation of microbial perchlorate reduction. *Environmental science & technology* **2007,** *41*, (5), 1740-6.
73. Gilman, M., Preparation of Cytoplasmic RNA from Tissue Culture Cells. In *Curr. Protoc. Mol. Biol.*, 2002; Vol. 58, pp 4.1.1-4.1.5.
74. Borgnia, M. J.; Kozono, D.; Calamita, G.; Maloney, P. C.; Agre, P., Functional reconstitution and characterization of AqpZ, the E. coli water channel protein. *Journal of molecular biology* **1999,** *291*, (5), 1169-1179.
75. Scatchard, G.; Hamer, W. J.; Wood, S. E., Isotonic Solutions. I. The Chemical Potential of Water in Aqueous Solutions of Sodium Chloride, Potassium Chloride, Sulfuric Acid, Sucrose, Urea and Glycerol at 25°1. *Journal of the American Chemical Society* **1938,** *60*, (12), 3061-3070.
76. Clinical Laboratory Medicine. In 2 ed.; McClatchey, K. D., Ed. Lippincott Williams & Wilkins: Philadelphia, PA, 2002; p 1677.
77. Thorneley, R. N. F., A convenient electrochemical preparation of reduced methyl viologen and a kinetic study of the reaction with oxygen using an anaerobic stopped-flow apparatus. *Biochimica et Biophysica Acta (BBA) - Bioenergetics* **1974,** *333*, (3), 487-496.

78. Matos, C. T.; Velizarov, S.; Crespo, J. G.; Reis, M. A., Simultaneous removal of perchlorate and nitrate from drinking water using the ion exchange membrane bioreactor concept. *Water research* **2006,** *40*, (2), 231-40.
79. Haefele, T.; Kita-Tokarczyk, K.; Meier, W., Phase Behavior of Mixed Langmuir Monolayers from Amphiphilic Block Copolymers and an Antimicrobial Peptide. *Langmuir* **2005,** *22*, (3), 1164-1172.
80. Heil, S. R.; Holz, M.; Kastner, T. M.; Weingartner, H., Self-diffusion of the perchlorate ion in aqueous electrolyte solutions measured by 35Cl NMR spin-echo experiments. *Journal of the Chemical Society, Faraday Transactions* **1995,** *91*, (12), 1877-1880.
81. Cowan, S. W.; Schirmer, T.; Rummel, G.; Steiert, M.; Ghosh, R.; Pauptit, R. A.; Jansonius, J. N.; Rosenbusch, J. P., Crystal structures explain functional properties of two *E. coli* porins. *Nature* **1992,** *358*, (6389), 727-33.

APPENDIX A

Anaerobic Growth Media

Ralph S. Tanner (RST) Basal Media for *Azospira oryzae* (ATTC BAA-33) Growth

RST Basal Medium	(L^{-1})
RST Mineral Stock Solution	20 ml
RST Trace Metal Stock Solution	10 ml
RST Vitamin Stock Solution	10 ml
TES buffer	4.6 g
$NaHCO_3$	1.0 g
Yeast extract	1.0 g
$NaCH_3COOH$	2.0 g
$NaClO_4$	1.0 g

Adjust pH to 7.2 with 10N NaOH

Volumes less than 100 ml:

Cap and crimp seal bottles
Exchange headspace 3 times with UHP N_2 (10 psi)
Autoclave 120°C 15 min

Volumes greater than 100 ml:

Autoclave 120°C 20 min uncapped
Cap and crimp seal bottles while hot
Using sterile cotton filters, exchange headspace 3 times with UHP N_2 (5 psi) while hot

The larger the volume the longer a vacuum should be applied to the media:

Less than 100 ml 30 min, 15 min and 5 min
Greater than 100 ml 1hr, 30 min, and 15 min (while hot)

Note: A 1L culture grown to an OD of ~0.35 at 600 nm will yield ~1 g of *A. oryzae* (wet weight).

RST Stock Solutions

RST Mineral Stock Solution	(L^{-1})
NaCl	40 g
NH_4Cl	50 g
KCl	5.0 g
KH_2PO_4	5.0 g
$MgSO_4 \cdot 7H_2O$	10 g
$CaCl_2 \cdot 2H_2O$	1.0 g

RST Trace Metal Stock Solution	(L^{-1})
Nitrilotriacetic acid (pH 6.0 w/ KOH)	2.0 g
$MnSO_4 \cdot 2H_2O$	1.0 g
$Fe(NH_4)_2(SO_4)_2 \cdot 6H_2O$	0.8 g
$CoCl_2 \cdot 6H_2O$	0.2 g
$ZnSO_4 \cdot 6H_2O$	0.2 g
$CuCl_2 \cdot 2H_2O$	20 mg
$NiCl_2 \cdot 6H_2O$	20 mg
Na_2SeO_4	20 mg
$Na_2WO_4 \cdot 2H_2O$	20 mg
$Na_2MoO_4 \cdot 2H_2O$	20 mg

RST Vitamin Stock Solution	(L^{-1})
Pyridoxine HCl	10 mg
Riboflavin	5.0 mg
Calcium pantothenate	5.0 mg
PABA	5.0 mg
Thioctic acid	5.0 mg
Niacinamide	5.0 mg
Biotin	2.0 mg
Folic acid	2.0 mg
Vitamin B_{12}	5.0 mg

APPENDIX B

Table 1: Summarizing Perchlorate Activity of Cell Lysate (CL), Soluble Protein Fraction (SPF) and Vesicles.

Cell Growth Date	Test Date	Sample	Activity (U/L)
6/8/2011	6/18/2011	Anaerobic CL Preparation	41680.7
6/8/2011	6/18/2011	Anaerobic CL Preparation	45927.2
6/8/2011	6/18/2011	Anaerobic CL Preparation	54407.147
6/8/2011	6/18/2011	Anaerobic CL Control	511.16
6/8/2011	6/18/2011	Anaerobic CL Control	367.34
6/8/2011	6/18/2011	Anaerobic CL Control	1206.27
6/8/2011	6/18/2011	Aerobic CL Preparation	40805.77
6/8/2011	6/18/2011	Aerobic CL Preparation	52687.18
6/8/2011	6/18/2011	Aerobic CL Preparation	45733.52
6/8/2011	6/18/2011	Aerobic CL Control	444.47
6/8/2011	6/18/2011	Aerobic CL Control	363.11
6/8/2011	6/18/2011	Aerobic CL Control	157.28
	6/18/2011	Perchlorate Only Control	94.51
	6/18/2011	Perchlorate Only Control	31.04
	6/18/2011	Perchlorate Only Control	47.92
1/27/2011	4/15/2011	10% Glycerol Stabilization of SPF	22928.41
1/31/2011	4/15/2011	10% Glycerol Stabilization of SPF	26671.43
2/18/2011	4/15/2011	10% Glycerol Stabilization of SPF	26728.589
1/27/2011	4/15/2011	10% Glycerol Stabilization of SPF Control	386.14
1/31/2011	4/15/2011	10% Glycerol Stabilization of SPF Control	354.95
2/18/2011	4/15/2011	10% Glycerol Stabilization of SPF Control	360.54
1/27/2011	4/15/2011	Stabilization of SPF	24363.16

Table 1 (cont.)

1/31/2011	4/15/2011	Stabilization of SPF	29931.54
2/18/2011	4/15/2011	Stabilization of SPF	25437.82
1/27/2011	4/15/2011	Stabilization of SPF Control	692.66
1/31/2011	4/15/2011	Stabilization of SPF Control	315.43
2/18/2011	4/15/2011	Stabilization of SPF Control	455.41
1/31/2011	7/29/2011	10% Glycerol Stabilization of SPF After 2 Days	18886.71
2/18/2011	7/29/2011	10% Glycerol Stabilization of SPF After 2 Days	19475.78
2/25/2011	7/29/2011	10% Glycerol Stabilization of SPF After 2 Days	17854.73
1/31/2011	7/29/2011	10% Glycerol Stabilization of SPF After 2 Days Control	455.41
2/18/2011	7/29/2011	10% Glycerol Stabilization of SPF After 2 Days Control	286.47
2/25/2011	7/29/2011	10% Glycerol Stabilization of SPF After 2 Days Control	261.68
1/31/2011	7/29/2011	Stabilization of SPF After 2 Day	9896.1
2/18/2011	7/29/2011	Stabilization of SPF After 2 Day	9884.4
2/25/2011	7/29/2011	Stabilization of SPF After 2 Day	8851.26
1/31/2011	7/29/2011	Stabilization of SPF Control After 2 Days	168.36
2/18/2011	7/29/2011	Stabilization of SPF Control After 2 Days	149.39
2/25/2011	7/29/2011	Stabilization of SPF Control After 2 Days	155.46
3/1/2011	9/14/2011	Protease Treatment SPF	3226.99
2/25/2011	9/14/2011	Protease Treatment SPF	2809.38
2/18/2011	9/14/2011	Protease Treatment SPF	3001.6545
3/1/2011	9/14/2011	Protease Treatment SPF Control	142.84
2/25/2011	9/14/2011	Protease Treatment SPF Control	118.67
2/18/2011	9/14/2011	Protease Treatment SPF Control	130.46

Table 1 (cont.)

3/1/2011	9/14/2011	No Protease Treatment SPF	4082.17
2/25/2011	9/14/2011	No Protease Treatment SPF	4403.62
2/18/2011	9/14/2011	No Protease Treatment SPF	4202.62
3/1/2011	9/14/2011	No Protease Treatment SPF Control	75.86
2/25/2011	9/14/2011	No Protease Treatment SPF Control	117.5
2/18/2011	9/14/2011	No Protease Treatment SPF Control	94.35
4/1/2011	2/1/2012	Protease Inhibitor SPF	2471.16
6/5/2011	2/1/2012	Protease Inhibitor SPF	2543.64
4/1/2011	2/1/2012	Protease Inhibitor SPF Control	309.8
6/5/2011	2/1/2012	Protease Inhibitor SPF Control	322.28
4/1/2011	2/1/2012	No Protease Inhibitor SPF	2936.43
6/5/2011	2/1/2012	No Protease Inhibitor SPF	2766.22
4/1/2011	2/1/2012	No Protease Inhibitor SPF Control	286.28
6/5/2011	2/1/2012	No Protease Inhibitor SPF Control	355.27
2/25/2011	7/29/2011	Lipid OmpF Vesicle	51.55
5/2/2011	11/21/2011	Lipid OmpF Vesicle	38.85
5/23/2011	12/18/2011	Lipid OmpF Vesicle	38.61
2/25/2011	7/29/2011	Lipid OmpF Vesicle Control	3.45
5/2/2011	11/21/2011	Lipid OmpF Vesicle Control	5.52
5/23/2011	12/18/2011	Lipid OmpF Vesicle Control	5.03
2/25/2011	7/29/2011	Lipid No OmpF	30.14
5/2/2011	11/21/2011	Lipid No OmpF	17.44
5/23/2011	12/18/2011	Lipid No OmpF	7.78
2/25/2011	7/29/2011	Lipid OmpF Vesicle Protease	54.57
5/2/2011	11/21/2011	Lipid OmpF Vesicle Protease	59.54
5/23/2011	12/18/2011	Lipid OmpF Vesicle Protease	30.25
2/25/2011	7/29/2011	Lipid OmpF Vesicle Protease Control	2.59
5/2/2011	11/21/2011	Lipid OmpF Vesicle Protease Control	1.49
5/23/2011	12/18/2011	Lipid OmpF Vesicle Protease Control	6.29

Table 1 (cont.)

6/5/2011	2/3/2012	Polymer OmpF Vesicle	64.96
2/2/2012	2/15/2012	Polymer OmpF Vesicle	70.22
3/18/2012	3/26/2012	Polymer OmpF Vesicle	76.8
6/5/2011	2/3/2012	Polymer No OmpF Vesicles	38.87
2/2/2012	2/15/2012	Polymer No OmpF Vesicles	50.73
3/18/2012	3/26/2012	Polymer No OmpF Vesicles	41.41
6/5/2011	2/3/2012	Polymer No OmpF No Detergent Vesicles	20.31
2/2/2012	2/15/2012	Polymer No OmpF No Detergent Vesicles	24.34
3/18/2012	3/26/2012	Polymer No OmpF No Detergent Vesicles	23.47
6/5/2011	2/3/2012	Polymer OmpF Protease Vesicles	62.29
2/2/2012	2/15/2012	Polymer OmpF Protease Vesicles	54.89
3/18/2012	3/26/2012	Polymer OmpF Protease Vesicles	64.51
6/5/2011	2/3/2012	Polymer No OmpF Protease Vesicles	43.65
2/2/2012	2/15/2012	Polymer No OmpF Protease Vesicles	41.66
3/18/2012	3/26/2012	Polymer No OmpF Protease Vesicles	30.14

APPENDIX C

Calculations of Theoretical Vesicle Activity. The activity of the vesicles was much lower than soluble protein fraction. To determine the possible causes of this reduction in activity, theoretical calculations of the vesicles' activity were performed with respect to 1) the total volume activity (TVA) restriction of the vesicle determined by the encapsulation volume of the perchlorate-reducing vesicles and 2) the diffusion limited activity (DLA) determined by the perchlorate diffusion across OmpF in the polymer membrane. Several assumptions went into these calculations and were included at appropriate points in the calculations

1. ENCAPSULATION VOLUME RESTRICTION ON ACTIVITY

The total volume activity (TVA) was calculated using Equation 3.

$$TVA = \frac{TEV * APF}{TVV} \quad \textbf{(1)}$$

Equation 3: Volume Restriction on Vesicle Activity.
The theoretical total volume activity (TVA) was calculated using the total vesicle encapsulation volume (TEV), the activity of the soluble protein fraction (APF), and the total suspension volume of vesicle (TVV) after preparation using size exclusion chromatography.

The TEV was calculated by determining the total number of vesicles (TNV) and the encapsulation volume of one vesicle (EV).

$$TEV = TNV * EV \quad \textbf{(2)}$$

The Total Number of Vesicles (TNV) was difficult to determine from dynamic light scattering results due to their small size. So, the TNV was calculated using the mass of polymer, the surface area (SA) of a polymer molecule, and the surface area of a vesicle. This calculation assumed that all polymer molecules were incorporated into vesicles. This assumption was made as the experiments were not designed to account for polymer lost during vesicle preparation which included extrusion and size exclusion.

$$\boldsymbol{TNV = \frac{polymer\ molecules * SA\ of\ polymer\ molecule}{SA\ of\ a\ Vesicle}} \quad \textbf{(3)}$$

The number of polymer molecules was determined from the experimental mass of polymer, 12 mg. This value was converted to the total number of polymer molecules using the gram formula mass of 11048 mg/mmol calculated from the polymer structure (Figure 3).

$$\boldsymbol{12.0 mg\ polymer * \frac{1 mmol}{11048 mg} * \frac{1 mol}{1000 mmol} = 1.09 * 10^{-6} mol\ polymer} \quad \textbf{(4)}$$

The total number of polymer molecules was calculated using the moles of polymer and Avogadro's number.

$$\boldsymbol{1.09 * 10^{-6} mol * 6.02 * 10^{23} \frac{molecules}{mol} = 6.56 * 10^{17} polymer\ molecules} \quad \textbf{(5)}$$

The surface area of a polymer molecule was 350 $Å^2$ [79]. This value was determined experimentally; however, the value was obtained from a reported range of values, 200 to 500 $Å^2$. In addition, the polymer used in the published experiment contained block number, $A_{16}B_{74}A_{16}$, which is smaller than the polymer used in the experiments of this thesis. The surface area of a

vesicle was determined using geometrical equation for the surface area of a sphere and the assumed diameter of 180 nm (a radius of 90 nm). The diameter of the vesicles was determined using dynamic light scattering. The radius was an average value and for these calculations, all vesicles are assumed to have a uniform vesicle diameter of 180 nm.

$$\mathbf{4 * \pi * (90.0nm)^2 * \frac{1Å^2}{(0.1nm)^2} = 1.02 * 10^7 Å^2/Vesicle} \qquad \mathbf{(6)}$$

The TNV was calculated using equation line (3).

$$\mathbf{\frac{6.56*10^{17} polymer\ molecules * 350\left(\frac{Å^2}{polymer\ molecule}\right)}{1.02*10^7\left(\frac{Å^2}{Vesicle}\right)} = 2.25 * 10^{13} Vesicles} \qquad \mathbf{(7)}$$

The encapsulation volume (EV) of a vesicle was determined from the geometrical equation of volume for a sphere. The inner diameter of the vesicle was used. The inner diameter of the vesicle was determined from light scattering and the thickness of the polymer, 15 nm. The inner diameter used in these calculations was 150 nm.

$$\mathbf{\frac{4}{3} * \pi * \frac{(75.0nm)^3}{Vesicle} * \frac{1*10^{-27}m^3}{1nm^3} * \frac{1000L}{1m^3} = 1.77 * 10^{-18} L/Vesicle} \qquad \mathbf{(8)}$$

From equation line (2), the TEV was calculated.

$$\mathbf{(1.77 * 10^{-18}) \frac{L}{Vesicle} * 2.25 * 10^{13} Vesicles = 3.98 * 10^{-5} L} \qquad \mathbf{(9)}$$

Having calculated the total encapsulation volume (TEV), the APF and TVV from equation line (1) was determined next. The APF was calculated assuming the encapsulation volume contained uniform activity similar to the soluble protein fraction. The activities from soluble protein fraction used to prepare the vesicle in experiments performed in this thesis ranged from 5000 to 15,000 U/L. For these calculations, the activity was assumed at 15,000 U/L in order to calculate a theoretical maximum. The most direct means of calculating vesicle concentrations was not available during these experiments. Since a method was not available, the total vesicle suspension volume (TVV) was used with the total number of vesicles to determine an approximate concentration. This value was obtained after vesicle preparation including extrusion and size exclusion chromatography. During size exclusion chromatography, the separation of vesicles from the soluble protein fractions resulted in an unknown dilution. However, the volume of the vesicle suspension was determined from size exclusion chromatography. This volume, TVV, was used to determine limitations of the total volume activity (TVA)

$$\boldsymbol{TVA = \frac{3.98 * 10^{-5} L * \left(15{,}000\left(\frac{U}{L}\right)\right)}{0.004 L} = 149\ U/L} \qquad \textbf{(10)}$$

2. PERCHLORATE DIFFUSION RESTRICTION ON ACTIVITY

The diffusion limiting activity (DLA) was calculated using Equation 4.

$$DLA = \frac{F * SAV}{TVV} \quad (11)$$

Equation 4: Diffusion Limiting Activity.
The diffusion limiting activity was determined using the flux of perchlorate (F), the surface area of the vesicles (SAV), and the total vesicle suspension volume (TVV).

$$F = -D * n * \frac{dC}{dx} \quad (12)$$

Equation 5: Fick's First Law for Diffusion.
The flux of perchlorate was determined from the diffusion coefficient (D), the porosity of the vesicles (n), and the perchlorate concentration gradient (dC/dx).

For perchlorate, the diffusion coefficient (D) was determined as 2.25 X 10^{-5} cm^2/s [80]. The equations were further adapted to account for the pore structure of the vesicles. Perchlorate should only be able to diffuse into the vesicles through pores. While data suggest that the vesicles were permeable through the polymer, for now, I assumed that flux can only occur though the OmpF. Also, I assumed flux of perchlorate into the pore was not hindered by steric effects. The calculations assumed 100% insertion efficiency of the 1:200 molar ratio of OmpF to polymer. Experiments were not designed to determine the insertion efficiency of the OmpF. The porosity of the vesicle, a unitless value, was determined from the ratio of OmpF surface area to vesicle surface area and molar ratio. The dimensions of the pore were given as 7Å by 11Å [81]. The surface area of the elliptical OmpF was 60.5 $Å^2$.

$$\frac{\boldsymbol{polymer\ molecule}}{\mathbf{350}\text{Å}^{\mathbf{2}}} * \frac{\mathbf{1}\ \boldsymbol{OmpF}}{\mathbf{200}\ \boldsymbol{polymer\ molecules}} * \frac{\mathbf{60.5}\text{Å}^{\mathbf{2}}}{\mathbf{1}\ \boldsymbol{OmpF}} = \mathbf{0.000864} \qquad \mathbf{(13)}$$

The concentration gradient (dC/dx) was determined by the perchlorate concentration used in the experiments (0.83 μmole/cm^3) over the radius of the vesicle. The radius of the vesicle was used rather than the thickness of the membrane to account for the laminar layer that surrounds the vesicle. The flux of perchlorate (F) was determined using equation line (12).

$$\frac{\mathbf{2.25}*\mathbf{10}^{-\mathbf{5}}\left(\frac{\boldsymbol{cm}^{\mathbf{2}}}{\boldsymbol{s}}\right)*\mathbf{0.000864}*\left(\mathbf{0.83}*\left(\frac{\boldsymbol{\mu mol}}{\boldsymbol{cm}^{\mathbf{3}}}\right)\right)}{\mathbf{9.00}*\mathbf{10}^{-\mathbf{6}}\boldsymbol{cm}} = \mathbf{.00179}\left(\frac{\boldsymbol{\mu mol}}{\boldsymbol{cm}^{\mathbf{2}}*\boldsymbol{s}}\right) \qquad \mathbf{(14)}$$

The flux of perchlorate was converted to μmoles of methyl viologen consumed per minute to make units consistent with previous activity values. Four moles of methyl viologen are required to convert perchlorate into chlorite. Chlorite exchanges electrons intramolecularly to form chloride and diatomic oxygen. Oxygen consumes an additional four moles of methyl viologen to form water. Together, perchlorate consumes eight moles of methyl viologen (MV).

$$\mathbf{0.00179}\frac{\boldsymbol{\mu mol}\ \boldsymbol{ClO_4^-}}{\boldsymbol{cm}^{\mathbf{2}}*\boldsymbol{s}} * \frac{\mathbf{8}\boldsymbol{\mu mol}\ \boldsymbol{MV}}{\boldsymbol{\mu mol}\ \boldsymbol{ClO_4^-}} * \frac{\mathbf{60}\boldsymbol{s}}{\boldsymbol{min}} = \mathbf{0.859}\frac{\boldsymbol{\mu mol}\ \boldsymbol{MV}}{\boldsymbol{min}*\boldsymbol{cm}^{\mathbf{2}}} \qquad \mathbf{(15)}$$

Having determined the flux of perchlorate (F), the total surface area of the vesicles was calculated using the surface area of one vesicle and the total number of vesicles as previously calculated in equation lines (6) and (7).

$$\mathbf{1.02} * \mathbf{10}^{\mathbf{7}}\frac{\text{Å}^{\mathbf{2}}}{\boldsymbol{Vesicle}} * \mathbf{2.25} * \mathbf{10}^{\mathbf{13}}\boldsymbol{Vesicle} * \frac{\mathbf{1}\boldsymbol{cm}^{\mathbf{2}}}{\mathbf{10}^{\mathbf{16}}\text{Å}^{\mathbf{2}}} = \mathbf{23,000}\boldsymbol{cm}^{\mathbf{2}} \qquad \mathbf{(16)}$$

The final calculation used equation line (11) to determine the activity of vesicles when considering diffusion of perchlorate into the vesicle.

$$\frac{0.859\frac{\mu mol}{min*cm^2}*\ 23000cm^2}{0.004L} = 4.94 * 10^6 U/L \qquad (17)$$

See the Discussion for comparison of the vesicle encapsulation and perchlorate diffusion limitations on perchlorate degradation.